

THE EFFECT OF ACID ADDITIVES ON CARBONATE ROCK WETTABILITY
AND SPENT ACID RECOVERY IN LOW PERMEABILITY GAS CARBONATES

A Thesis

by

MEHRNOOSH SANEIFAR

Submitted to the Office of Graduate Studies of
Texas A&M University
in partial fulfillment of the requirements for the degree of

MASTER OF SCIENCE

August 2011

Major Subject: Petroleum Engineering

THE EFFECT OF ACID ADDITIVES ON CARBONATE ROCK WETTABILITY
AND SPENT ACID RECOVERY IN LOW PERMEABILITY GAS CARBONATES

A Thesis

by

MEHRNOOSH SANEIFAR

Submitted to the Office of Graduate Studies of
Texas A&M University
in partial fulfillment of the requirements for the degree of

MASTER OF SCIENCE

Approved by:

Co-Chairs of Committee, Mashhad Fahes
Alfred D. Hill

Committee Member, Reza Langari
Head of Department, Stephen A. Holditch

August 2011

Major Subject: Petroleum Engineering

ABSTRACT

The Effect of Acid Additives on Carbonate Rock Wettability and Spent Acid Recovery
in Low Permeability Gas Carbonates. (August 2011)

Mehrnoosh Saneifar, B.S., Texas A&M University at Qatar

Co-Chairs of Advisory Committee: Dr. Mashhad Fahes
Dr. Alfred D. Hill

Spent acid retention in the near-wellbore region causes reduction of relative permeability to gas and eventually curtailed gas production. In low-permeability gas carbonate reservoirs, capillary forces are the key parameters that affect the trapping of spent acid in the formation. Capillarity is a function of surface tension at the gas-liquid interface and contact angle of the fluids in the rock. To weaken capillary forces, surface tension should be low and contact angle should be large. This work provides a comprehensive study on the effect of various common acid additives on carbonate rock wettability, and surface tension and contact angle, as the main parameters that control capillarity. Surface tension and contact angle experiments were conducted using Drop Shape Analysis (DSA) instrument at high temperature and pressure. Core flood experiments were also conducted to study the overall impact of the acid additives on wettability by analyzing irreducible fluid saturation in the rocks before and after spent acid exposure. Spontaneous water imbibition was conducted in each case to check for permanent or long-term wettability change as a result of using these additives.

Acid additives such as methanol and corrosion inhibitors reduced both surface tension and contact angle. Iron control agents had no impact on surface tension, however, they decreased contact angle at the lower concentration used. Formic and acetic acids did not affect the surface tension, but they had a reducing impact on the contact angle.

According to the core flood experiment results, formic acid decreased irreducible fluid saturation whereas methanol increased irreducible fluid saturation. On the other hand, the fluorochemical surfactant tested changed the rock wettability into more gas wetting. Use of this chemical would help in recovering spent acid.

The results of the spontaneous water imbibition tests showed that organic acids and iron control chemicals did not have a permanent impact on wettability of the rocks. However, the wettability change as a result of using fluorochemical surfactant would persist for a long time as this chemical forms a film on the rock surface.

DEDICATION

To my mom and dad who have always supported me and taught me to be strong.

Love you both very much.

ACKNOWLEDGEMENTS

I would like to thank my committee chair, Dr. Fahes, for her continuous encouragement and guidance throughout the course of this research. I would also like to express my gratitude to Dr. Hill for his support and contribution to this study. In addition, I would like to extend my appreciation to Dr. Nasr-El-Din for his guidance and support in this work.

Thanks also go to my friends and colleagues at Texas A&M University in both College Station and Qatar, who have supported me throughout this journey.

I also want to extend my gratitude to the Qatar National Research Fund (QNRF) for providing the funding for this research, and the Sponsors of Middle East Carbonate Stimulation Research Program (MECS) for supporting this work.

NOMENCLATURE

σ	Surface Tension
θ	Contact Angle
ϕ	Porosity
μ	Viscosity
g	Gravitational Acceleration
k	Permeability
k_a	Absolute Permeability
k_g	Gas Effective Permeability
k_l	Liquid Effective Permeability
k_{rg}	Liquid Relative Permeability
k_{rl}	Liquid Relative Permeability
q	Flow Rate
R_m	Mean Pore Radius
P_1	Inlet Pressure
P_2	Outlet Pressure
P_c	Capillary Pressure
P_{st}	Reservoir Static Pressure
P_w	Wetting phase Pressure
P_{nw}	Non-wetting phase pressure
S_l	Liquid Saturation

V_b	Bulk Volume
V_d	Dead Volume
V_m	Matrix Volume
V_p	Pore Volume
V_s	Volume of Spacers
W_{ai}	Initial Apparent Weight
W_{af}	Final Apparent Weight
W_{ri}	Initial Real Dry Weight
W_{rf}	Final Real Dry Weight

TABLE OF CONTENTS

	Page
ABSTRACT	iii
DEDICATION.....	v
ACKNOWLEDGEMENTS	vi
NOMENCLATURE	vii
TABLE OF CONTENTS.....	ix
LIST OF FIGURES	xi
LIST OF TABLES.....	xiv
CHAPTER	
I INTRODUCTION AND LITERATURE REVIEW	1
Matrix Acidizing.....	1
Wormholes	3
Spent Acid Formation	5
Capillarity and Spent Acid Retention	6
Contact Angle and Wettability	9
Relative Permeability Measurements	11
Acid Additives.....	13
Objectives.....	17
II EXPERIMENTAL SETUP AND PROCEDURE.....	18
Materials.....	18
Equipment	22
Procedure.....	28
III RESULTS AND DISCUSSIONS	39
Surface Tension Experiments.....	39
Contact Angle Experiments.....	46
Spontaneous Water Imbibition and Irreducible Saturation Tests...	51

CHAPTER	Page
IV CONCLUSIONS	61
REFERENCES	65
VITA	69

LIST OF FIGURES

	Page
Fig. 1 A schematic diagram of near-wellbore zone after spent acid invasion	5
Fig. 2 A sketch of pores and grains in the rock, demonstrating the tendency of the wetting fluid (water) to occupy the small pore spaces and the non-wetting fluid (gas) to occupy the large pore spaces in gas reservoirs	7
Fig. 3 Wettability as defined by contact angle; the contact angle over 90 degrees is achieved in the case of gas-wetting and a contact angle less than 90 degrees is achieved in the case of water-wetting	10
Fig. 4 Typical gas-water relative permeability plot	11
Fig. 5 Gas-water relative permeability measurements versus water saturation for Berea sandstone	12
Fig. 6 Chemical structures of common acid additives	15
Fig. 7 Flow setup used for coreflood tests	23
Fig. 8 Spontaneous liquid imbibition setup	24
Fig. 9 A schematic diagram of the HT/HP pendant drop instrument	26
Fig. 10 Helium porosimeter	27
Fig. 11 Methanol Extraction Equipment	28
Fig. 12 Typical gas-water relative permeability plot; corresponding relative permeability end points	33
Fig. 13 Pendant drop image extracted and digitized by the image analysis software. The top two horizontal lines are used to estimate the volume of the capillary tube and the bottom line is used to determine top of the droplet	36
Fig. 14 Sessile drop image extracted and digitized by the image analysis software	37

	Page
Fig. 15 Spending formic acid in a beaker by adding chunks of carbonate rock	38
Fig. 16 Effect of temperature on surface tension of spent HCl acid with no additives at 1000 psi	40
Fig. 17 Effect of methanol on surface tension of spent acid at 1000 psi	41
Fig. 18 Effect of inhibitor I on surface tension of spent acid at 1000 psi	42
Fig. 19 Effect of inhibitor II on surface tension of spent acid at 1000 psi	42
Fig. 20 Effect of HEDTA on surface tension of spent acid at 1000 psi	43
Fig. 21 Effect of GLDA on surface tension of spent acid at 1000 psi	44
Fig. 22 Effect of formic acid on surface tension of spent acid at 150 °C and 1000 psi	45
Fig. 23 Effect of acetic acid on surface tension of spent acid at 150 °C and 1000 psi	45
Fig. 24 Stabilized spent acid droplet after 2 hours.....	46
Fig. 25 Effect of methanol on contact angle of spent acid at 100 °C & 1000 psi	47
Fig. 26 Effect of acetic acid on contact angle of spent acid at 100 °C & 1000 psi	48
Fig. 27 Effect of formic acid on contact angle of spent acid at 100 °C & 1000 psi	48
Fig. 28 Effect of HEDTA on contact angle of spent acid at 100 °C & 1000 psi	49
Fig. 29 Effect of GLDA on contact angle of spent acid at 100 °C & 1000 psi	50

	Page
Fig. 30 Sessile drop images of spent acid with 0.2 wt.% inhibitor I for contact angle analysis	51
Fig. 31 Spontaneous water imbibition for untreated and treated core samples with 15 wt.% and 28 wt.% spent HCl	52
Fig. 32 Spontaneous water imbibition for untreated and treated ILS21 with 5 wt.% formic acid in 15 wt.% spent HCl acid	56
Fig. 33 Spontaneous water imbibition for untreated and treated ILS23 with 5 wt.% methanol in 15 wt.% spent HCl acid	57
Fig. 34 Spontaneous water imbibition for untreated and treated ILS6 with 0.3 wt.% sodium erythorbate in 15 wt.% spent HCl acid	57
Fig. 35 Spontaneous water imbibition for untreated and treated ILS11 with 0.3 wt.% EDTA in 15 wt.% spent HCl acid	58
Fig. 36 Spontaneous water imbibition for untreated and treated MR12 with 4 wt.% fluorochemical surfactant in 15 wt.% spent HCl acid	59
Fig. 37 Effect of wettability change on gas relative permeability and irreducible liquid saturation in case of using 1% fluorochemical surfactant in 15 wt.% spent HCl acid	60

LIST OF TABLES

	Page
Table 1 List of core samples used and their properties	19
Table 2 List of acid additives used and their concentrations in 15 wt.% spent HCl acid	21
Table 3 List of the equipment, brands and models	22
Table 4 List of all core samples used, the treatments and experiments conducted in each case	54
Table 5 Results of irreducible liquid saturation for ILS21 and ILS23	55

CHAPTER I
INTRODUCTION AND
LITERATURE REVIEW

Matrix Acidizing

Near-wellbore permeability is normally impaired during drilling and completion, due to invasion of solid particles entrained in the fluids used in these operations. As a result of this reduction in permeability, also known as formation damage, the productivity of the well is negatively affected. Successful matrix acidizing treatments can overcome this damage and increase the well productivity even beyond that of the undamaged reservoir (Economides *et al.* 1994). Acid is injected at a pressure lower than the natural fracture gradient and dissolves near-wellbore damage, connecting the wellbore with the undamaged original permeability of the reservoir.

Matrix acidizing can also be used to improve formation permeability in undamaged wells. The purpose of this treatment is to accomplish, more or less, radial acid penetration deep into the formation to increase formation permeability around the wellbore. This would lead to a negative skin effect and an enhancement in hydrocarbon flow near the wellbore.

Matrix acidizing is most useful when fracture acidizing is undesirable, such as when a shale break or other natural boundary must be retained to prevent water or gas

This thesis follows the style of *SPE Production & Operations*.

production or where fracture acidizing is unsuccessful, such as in soft chalk formations (Fredd and Fogler 1998).

To select a well as the right candidate for matrix acidizing different factors must be considered. The well should have a high skin factor, high undamaged permeability and a shallow depth of damage. If there is no skin damage, a matrix treatment in carbonates will stimulate natural production as much as two times. If the natural undamaged permeability is low, acid fracturing is more suitable (Schechter 1992).

Selection of the acid for matrix treatment depends on how it would react with the formation rock, the solubility of the reaction products and the handling characteristics of the acid itself. Hydrochloric acid (HCl) is used as the main stimulation fluid for acid fracturing and matrix acidizing in carbonate reservoirs. HCl is cheap, has a high rock-dissolving power, and the reaction products are usually soluble. (Schechter 1992).

On the other hand, the high reaction rate of HCl with carbonate rock means that the acid does not penetrate very far into the formation before it is spent. Acidizing using HCl acid is therefore of limited effectiveness in treatments where deep penetration is needed. For these cases, there are several alternative techniques that can be used. Addition of a polymer to acid increases acid viscosity. Consequently the diffusion rate of acid and acid/rock reaction products is reduced, and thus the overall acid-spending rate is decreased. Emulsified acid is another system that lowers acid reactivity by reducing acid diffusion rate. HCl acid is generally used in these systems as the internal phase of an oil external emulsion. Emulsified acid combines a relatively high rock-dissolving power with a low acid/rock reaction rate (Buijse *et al.* 2004). Another approach is to use

other, less aggressive acid types, such as organic acids (Nasr-El-Din *et al.* 2004). Organic acids, mainly acetic and formic acid, are added to HCl in order to slow down acid spending on carbonate rock and provide deeper penetration and improved stimulation. Formic and acetic acids are common organic acids that are used with 15 wt.% HCl at concentrations of 9 and 13 wt.%, respectively. At higher concentrations there would be a potential for precipitation of reaction products of the acids with the carbonate rock, calcium formate and calcium acetate, since the reaction between organic acids and carbonate is reversible (Nasreldin 2004). In recent years, other alternatives have been developed; Aminocarboxylic acids, long-chained carboxylic acids, and chelating agents such as GLDA can be used as effective stimulation fluids (Huang *et al.* 2003).

In this work we will only study the conventional carbonate acidizing with 15 wt.% HCl and common acid additives.

Wormholes

In carbonates, dissolution of rock matrix in acid is not uniform as in sandstone acidizing. Natural heterogeneity of the porous medium in addition to inconsistent dissolution of rock materials results in the formation of infinitely permeable flow channels known as wormholes. This highly selective pattern of dissolution dissolves certain parts of the medium creating wormholes whereas other parts remain unaffected.

During stimulation, acid tends to flow through regions of highest permeability. These initial flow patterns are quickly extended and widened by the dissolution of matrix materials. A dominant channel quickly forms and continues to propagate. The structure

of these wormholes strongly depends on the rates of mass transfer and surface reaction, which may vary considerably among different acid/rock systems, as well as flow geometry and injection rate (Shukla 2003).

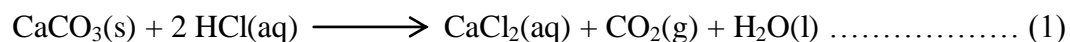
Wormholes induce a negligible pressure drop through the stimulated region by enlarging the pore-throats. As a result of this, they provide almost no resistance to flow and ultimately carry all the injected fluids. Hence, the impact of acidizing on the skin factor and the damage removal process strongly depends on the wormhole pattern, wormhole density, and wormhole penetration depth (Shukla 2003).

Consequently, the most efficient process is the one that results in narrower wormholes with a minimum of side-branching. This process will propagate the wormholes a given distance and enhance the near wellbore permeability to the greatest depth with the smallest volume of acid (Shukla 2003).

Many studies have been previously conducted on modeling the wormholing process in carbonate acidizing (Buijse and Glasbergen 2010; Huang 2000; Fredd and Fogler 1998; Daccord 1989; Bazin 1996; Wang 1993; Fredd and Fogler 1999; Bazin and Abdulahad 1999; Hung 1989; Wang 1993; Schechter 1992). These models can be used to better understand the acidizing mechanism in carbonates in order to achieve an effective stimulation job.

Spent Acid Formation

As a result of the reaction between HCl acid and carbonate rocks, spent acid which is mainly water and salt, CaCl₂, is produced. **Eq. 1** is the chemical reaction between calcite mineral (CaCO₃) and HCl acid.



The wormholing process creates a stimulated region around the well with a very high permeability, and consequently eliminates any effects of damage around the well. However, once spent acid is formed, it penetrates deeper beyond the stimulated zone. Therefore, there will be an extensive region of rock containing spent acid ahead of the wormholes, as shown in **Fig. 1**.

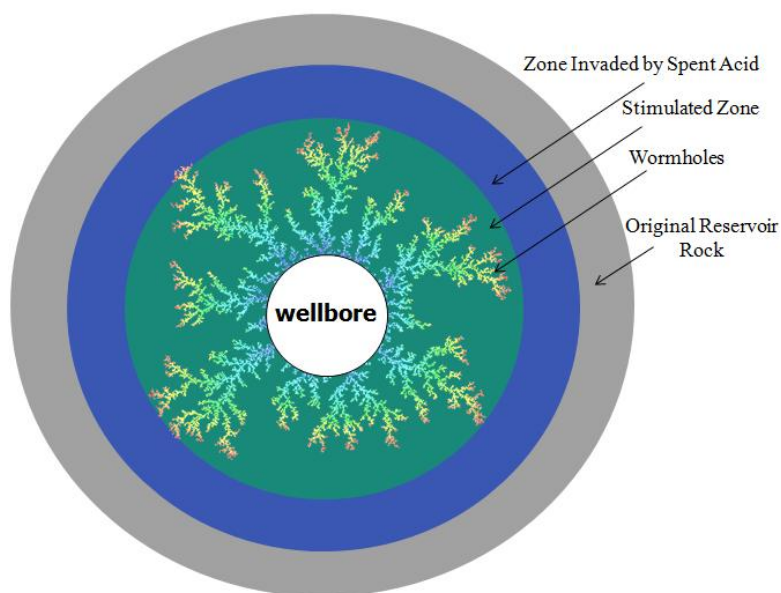


Fig. 1—A schematic diagram of near-wellbore zone after spent acid invasion.

A significant amount of spent acid is usually trapped in this zone and cannot be recovered after acidizing. This is a similar problem to water blockage occurring in low permeability gas reservoirs as the spent acid is constituted mostly of water. Accumulation of spent acid in the near-wellbore region causes a reduction in gas relative permeability and consequently results in curtailed gas production.

Capillarity and Spent Acid Retention

Capillary pressure forces are the main reason behind aqueous phase trapping at pore-throats in low permeability gas reservoirs. In a porous media, capillary pressure is normally expressed as the pressure difference between the wetting (usually water in gas reservoirs) and non-wetting (gas) phases, **Eq. 2**. They are also a function of surface tension at the gas-water interface and pore-throat radii, as expressed in the following equation:

$$P_c = P_{nw} - P_w \dots\dots\dots (2)$$

$$= \frac{2\sigma\cos\theta}{R_m}$$

P_c , P_{nw} and P_w are capillary, non-wetting and wetting phase pressures, respectively; σ is the surface tension (interfacial tension at the liquid-vapor interface), R_m is the mean pore radius and θ is the contact angle between the liquid phase and the rock surface (Bennion 1996).

As can be seen from **Eq. 2**, the effect of capillary forces is more pronounced in low permeability reservoirs, because the smaller the pore-throat radius, the larger the capillary pressure is. Consequently, the trapping effects are more significant in low permeability formations. In addition to that, the wetting phase (water) generally occupies

the smaller pore spaces whereas non-wetting phase (gas) occupies the larger pore spaces. Thus the mobility of spent acid or water is generally lower in comparison to gas in gas reservoirs. This mechanism is illustrated in **Fig. 2**.

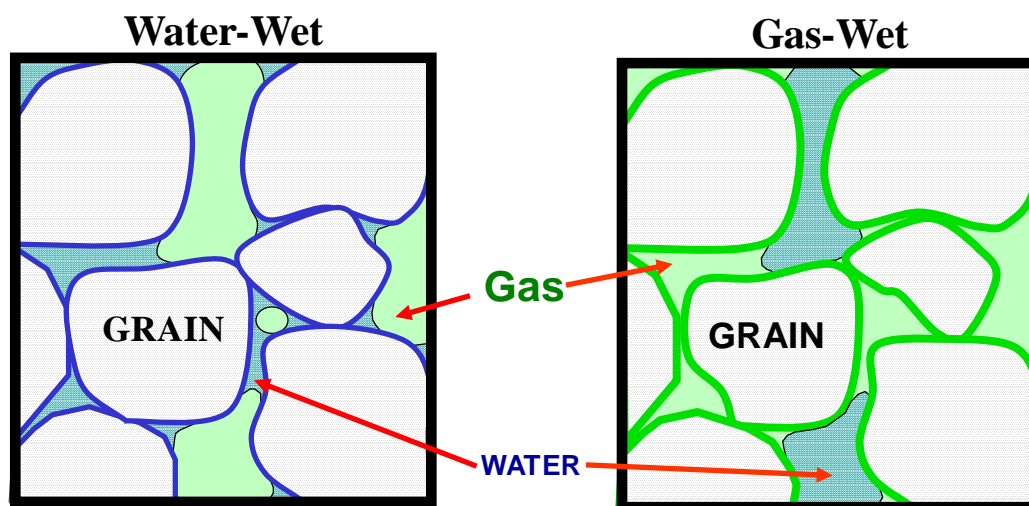


Fig. 2—A sketch of pores and grains in the rock, demonstrating the tendency of the wetting fluid (water) to occupy the small pore spaces and the non-wetting fluid (gas) to occupy the large pore spaces in gas reservoirs.

The actual pressure drop required for mobilizing the trapped spent acid or water in low permeability gas reservoirs is given by the difference between the reservoir static pressure P_{st} and the capillary pressure P_c (Travaloni- Louvise 1990).

$$\Delta p = P_{st} - P_c \dots\dots\dots (3)$$

According to **Eq. 3**, in order to impose the greatest pressure drop for producing the spent acid droplets capillary pressure must be minimized. For this to be achieved, as evident from **Eq. 2**, surface tension must be small and contact angle must be large. This implies that the rocks should be of a non-wetting phase relative to the fluid that is

flowing through them. Therefore in order to remove the trapped spent acid which is mainly water, rocks are preferred not to be water wet.

Since the original wettability in most gas reservoirs is water-wetting, addition of a chemical that alters the wettability to gas- or intermediate-wetting will be useful. Penny (1983) has studied gas–water–rock systems, in which the surfactant used in fracturing causes wettability change and increase in the productivity by two to three times more than the conventionally fractured wells. Li and Firoozabadi (2000) and Tang and Firoozabadi (2002) have also found that using a 3M-manufactured surfactant FC-722 and FC-759 in their wettability change in gas-condensate reservoirs results in intermediate-wet conditions, which leads to significant changes in imbibition rates and gas relative permeability. In recent years, a new chemical treatment has also been developed to facilitate the problem of liquid blockage in low permeability gas reservoirs (Butler 2009). In this treatment a non-ionic polymeric fluorinated surfactant is used in a brine tolerant solvent. The surfactant is non-reactive but interacts with the surface of the rocks under reservoir conditions to alter the wettability of the surface to less water-wetting. This change in the wettability causes an increase in gas relative permeability and enhancement in gas production.

Furthermore, low surface tension at the liquid-vapor interface is helpful in removing the trapped spent acid. An extensive study was done in the past to address the water blockage problem in low permeability gas reservoirs by reducing surface tension. Alcohols (Travaloni Louvisse 1990), surfactants (Hall 1975) and mutual solvents (King

and Lee 1988) such as ethylene glycol monobutylether (EGMBE) have shown great potential in reducing surface tension and great success in removing water blockage.

The process of spent acid recovery is a complex function of rock wettability and surface-active properties of the fluids involved. These rock and fluid properties can in fact be changed in a direction to optimize spent acid recovery and consequently improve the productivity of the wells.

Previous studies have also been done on the surface tension of various acid additives in live HCl acid (Randles and Schiffrin 1965; King and Lee 1988; Travaloni-Louvisse 1990; Weissenborn and Pugh 1996; Dabbousi 1999; Nasr-El-Din 2004). However, to the best of the author's knowledge, there is no study available on the surface tension of spent HCl acid with additives.

Contact Angle and Wettability

Contact angle is used to determine the wetting behavior of two immiscible fluids on a solid surface. Fluids are considered to be wetting if their contact angle with the surface is less than 90° and they are considered non-wetting if the angle is greater than 90° . For the case of spent acid trapping in gas carbonate reservoirs, a three-phase system is involved; the solid surface of the rock, the spent acid (water) and the gas. Wettability of the solid surface is thus defined based on the contact angle that the liquid interface makes with the surface as shown in **Fig. 3**.

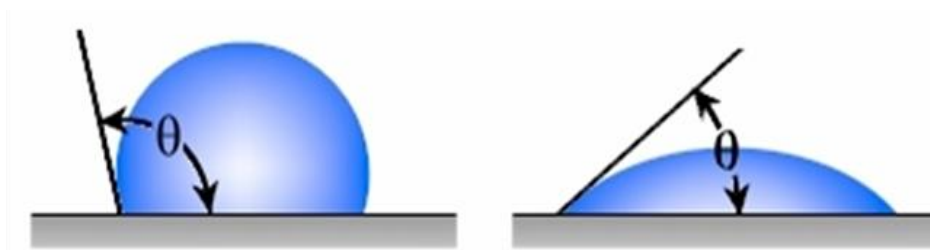


Fig. 3—Wettability as defined by contact angle; the contact angle over 90 degrees is achieved in the case of gas-wetting and a contact angle less than 90 degrees is achieved in the case of water-wetting.

When the contact angle (θ) is higher than 90° , the surface is preferentially gas wet; when it is less than 90° , the surface is water wet. A contact angle between 75° - 100° is usually known as intermediate wetting.

Because of the spreading effect and the capillary forces, the wetting phase tends to occupy the small pore spaces and have a low mobility compared to the non-wetting phase. In low permeability gas reservoirs, the capillary forces are very strong and trapping of spent acid is a common problem. The acid additives that are injected with acid into the reservoir can affect the wettability of the rocks both positively and negatively. The wettability changes to less water-wetting would result in better recovery of spent acid and higher gas rates. On the other hand, if the spent acid changes the wettability to strongly water-wetting, the result will be more spent acid trapping and ultimately reduction in gas productivity. It is very important to understand that the impact of acid additives on wettability of the rocks before acidizing can either favorably or unfavorably affect the spent acid recovery and gas production.

To the best of the author's knowledge, there is no study available on the effect of spent HCl acid with additives on the wettability of carbonate rocks.

Relative Permeability Measurements

Relative permeability measurements are used to identify the relative amounts of fluids that will flow through the formation when more than one fluid is present. A typical example of a gas-water relative permeability plot is shown in **Fig. 4**, where relative permeability measurements for water and gas are plotted against the wetting phase (water) saturation. When water saturation decreases gas relative permeability increases until it reaches irreducible water saturation. At this saturation, strong capillary forces trap water droplets and as a result, no more water can be recovered. The highest relative permeability to gas is achieved at irreducible water saturation.

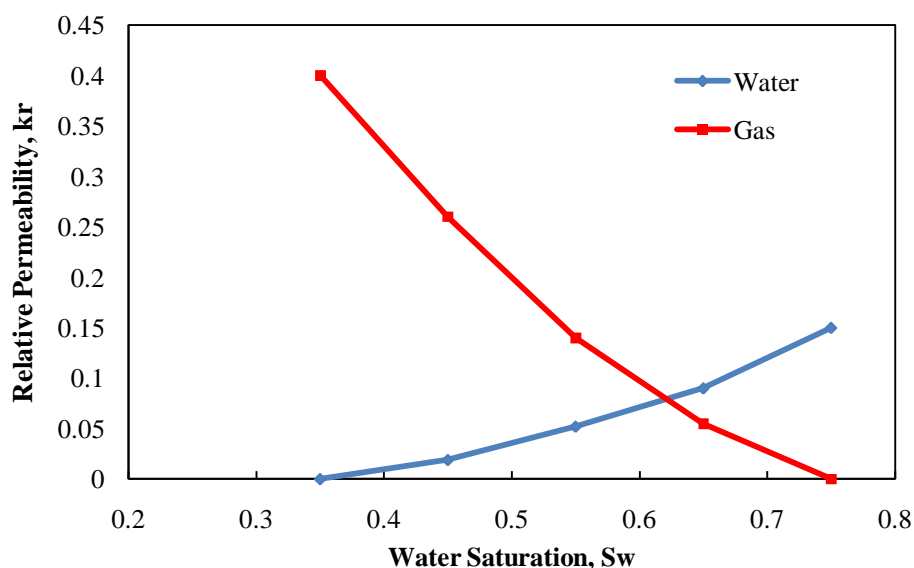


Fig. 4—Typical gas-water relative permeability plot.

The capillary forces are very strong in the near-wellbore zone invaded by spent acid. Therefore, the irreducible water or spent acid saturation is usually high. Alcohols that

reduce surface tension or surfactants that alter the wettability to less water-wetting can help in weakening the capillary forces and achieving lower irreducible water saturation.

Previous studies have shown that wettability change to intermediate wetting would reduce the irreducible water saturation allowing for less water blockage and consequently higher gas rates (Anderson 1987; Bennion 2000; Fahes and Firoozabadi 2007; Tang and Firoozabadi 2002). **Fig. 5** shows the relative permeability plots for gas and water from the study conducted by Tang and Firoozabadi (2002). This plot illustrates that change in wettability to intermediate-wetting causes a reduction in irreducible water saturation, in this case from 45% to 15% and an increase in gas relative permeability, from 0.3 to 0.8.

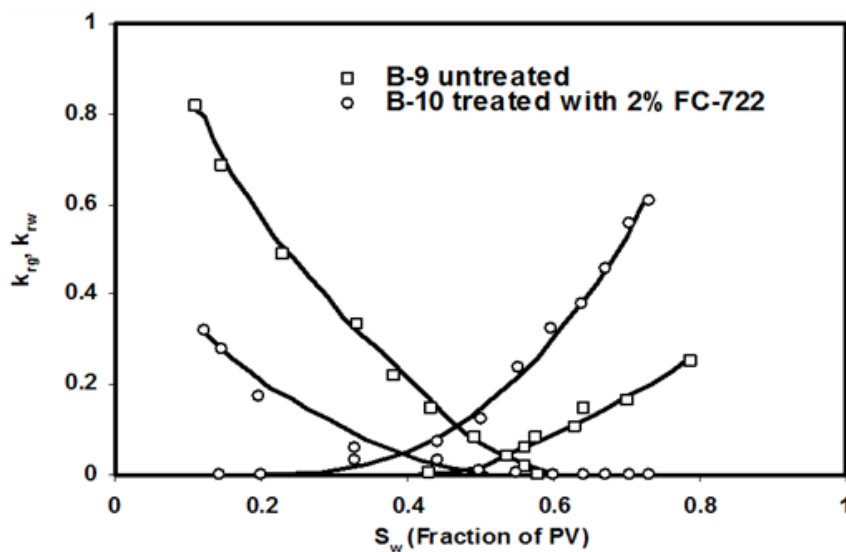


Fig. 5—Gas-water relative permeability measurements versus water saturation for Berea sandstone (Tang and Firoozabadi 2002).

If the chemicals that are injected with the acid into the well alter wettability to strong water-wetting or increase the surface tension, capillary forces will be stronger. This will cause more trapping, less spent acid recovery, and consequently curtailed gas production. On the other hand, if these acid additives have the reverse impact, they will actually result in an enhancement in gas production. Thus, it is necessary to conduct a thorough study on the effect of acid additives on capillary pressure forces before any acid job.

Acid Additives

Various acid additives are injected along with HCl when stimulating carbonates for different purposes. Due to the highly corrosive nature of HCl, corrosion inhibitors are always added to the acid. They are used in order to protect iron and steel in well tubulars, mixing tanks, coiled tubing and other metallic equipment from acid attacks. They must remain effective under reservoir pressure and temperature for the duration of the treatment and must not react with the acid itself. The commercial inhibitors used in acid stimulations are complex chemical substances but normally contain alkyl or alkylaryl nitrogen compounds (quaternary amines), and acetylenic alcohols (Frenier 1988). Cationic amines protect the metal surfaces by forming a film, and acetylenic alcohols protection is by polymerization and formation of barrier protective layers (Hellberg 2011).

In high temperature reservoirs, corrosion inhibitors cannot give adequate protection to low-carbon steels. Therefore, additional compounds called inhibitor intensifier are added to enhance the performance of the main corrosion inhibitor (Al-

Mutairi 2005). Formic acid is a common inhibitor intensifier that protects metal surfaces by undergoing a dehydration reaction to form water and carbon monoxide (CO), **Eq. 4** (Cassidy 2007). The carbon monoxide bubbles accumulate on the metal surfaces and protect them from corrosion.



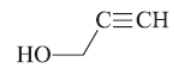
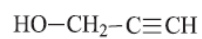
As previously mentioned, organic acids, like formic and acetic acids, are also used to slow down the acid-rock reaction rate and to provide deeper penetration and improved stimulation (Nasr-El-Din 2003).

Mutual solvents and alcohols are often used in acidizing to reduce surface tension of the fluids. Mutual solvents provide great solvency of hydrocarbon materials. Therefore in oil wells, they are used in acid pre-flushes to remove any oil films remaining on the surfaces. In addition they can be used in acid post-flushes to recover the original wettability of the rocks if changed by surfactants injected in the acid (King and Lee 1988). Mutual solvents are also used to minimize adsorption of the corrosion inhibitor onto reservoir rocks (Hall, 1975).

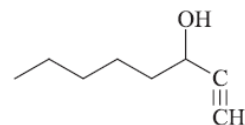
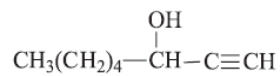
Iron control chemicals are another category of acid additives that are often added to prevent precipitation of ferric hydroxide in spent acid. Examples of iron control agents are chelating agents (EDTA, GLDA, HEDTA, etc.), citric acid and erythorbic acid. **Fig. 6** illustrates the chemical structures of the acid additives discussed above.

Corrosion Inhibitors

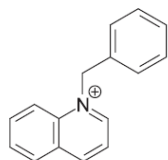
Propargyl Alcohol:



1-Octyn-3-ol:

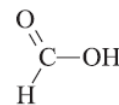


Benzylquinolinium Chloride:



Organic acids

Formic Acid:



Acetic Acid:

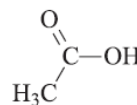
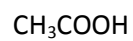
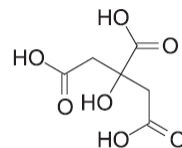
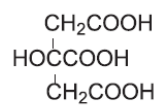


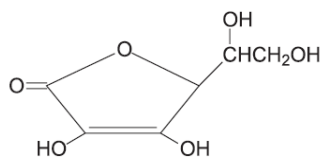
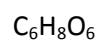
Fig. 6—Chemical structures of common acid additives (Nasr-El-Din 2004).

Iron Control Agents

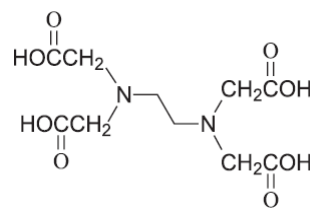
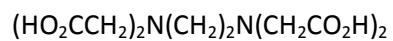
Citric Acid:



Erythorbic Acid:



EDTA:



Mutual Solvent

EGMBE:

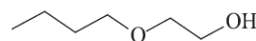
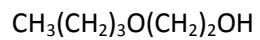


Fig. 6—Continued.

Objectives

The main objective of this work is to evaluate the effect of various common acid additives on carbonate rock wettability and consequent recovery of trapped spent acid in low permeability gas carbonate reservoirs. This includes studying the effect of these additives on the surface tension and contact angle as the main parameters that control capillarity.

CHAPTER II
EXPERIMENTAL SETUP
AND PROCEDURE

Materials

Rocks

Indiana limestone has been used as reference carbonate material in the research area by the petroleum industry for so many years. This rock type is formed in a shallow inland sea during Mississippian time. It is a calcite cemented grainstone formed from fossil fragments (specifically bryozoans, echinoderms, foraminifers, brachiopods and molluscs) and concentrically lamellar calcium carbonate particles named oolites. It is made up of the mineral calcite by 99% and has a small amount of other minerals (1%) (Churcher 1991).

Indiana limestone cores in lengths of 3 and 6 inches, and diameter of 1 inch were used in this study. The permeability of these cores ranged from 0.8 to 13 md and their porosity ranged from 10 to 16 vol.%. Core samples with similar properties were selected to ensure consistency in the study. A list of all the core samples used and their properties is provided in **Table 1**.

Core Sample	Length(in)	Porosity (vol.%)	Permeability (md)
MR10	3	11.03	10.40
MR11	3	10.94	8.70
MR12	3	11.81	13.70
MR33	3	11.40	7.50
ILS6	6	15.39	2.21
ILS11	6	10.31	0.80
ILS21	6	15.91	2.77
ILS23	6	15.04	2.89

Calcite Crystal Chips for Contact Angle Experiments

In order to obtain valid and accurate contact angle results extreme experimental care is required when conducting these experiments. Contact angle hysteresis can be due to roughness and/or heterogeneity of the solid surface used. To minimize the hysteresis due to roughness, solid surfaces can be polished and smoothed. To assure a homogeneous surface, crystals are a better option in comparison to rock substrates.

In this study, contact angle experiments were performed on 2×1 inch calcite crystal chips. Calcite crystals were further preferred to carbonate substrates because they are 100% impermeable and would assure a stable static droplet. The instability of a droplet while getting imbibed in the rock would lead to inaccurate contact angle measurements. The crystal chips were polished using sand paper (300-mesh) in order to prepare a smooth surface for the experiment.

Fluids

Distilled water was used as the liquid phase, in core flood experiments, spontaneous water imbibition, preparation of spent acid solution, calibration, and cleaning the equipment.

Compressed nitrogen gas (N_2) of 99.9% purity was used as the gas phase. Nitrogen is an inert gas, safe to use in the laboratory and easy to obtain in compressed form. Nitrogen was specifically used in permeability measurements, gas injection to obtain irreducible liquid saturation, surface tension and contact angle experiments.

Pure helium gas (He) was used in the porosimeter for porosity measurements. Helium is widely used for porosity measurements, because it is an inert gas with low absorption and high diffusivity rate.

Calcium Chloride ($CaCl_2$) was used to prepare 15 wt.% spent HCl acid, in proportional amounts according to **Eq. 1**.

Several common acid additives were used in the contact angle, the surface tension and some of the core flood experiments. **Table 2** lists these additives and their concentrations in spent acid.

Table 2—List of acid additives used and their concentrations in 15 wt.% spent HCl acid

Acid Additives	Concentration (wt.%)
Methanol	5, 30
EGMBE	5, 10, 30
Acetic Acid	1-30
Formic Acid	1-30
HEDTA	0.03, 0.3
GLDA	0.03, 0.3
EDTA	0.3
Sodium Erythorbate	0.3
Fluorochemical surfactant	1, 4
Inhibitor I	0.2, 2
Inhibitor II	0.2, 2

Ethylene glycol monobutylether (EGMBE) was used as the mutual solvent. Concentrated acetic and formic acids were tested as the common organic acids used in carbonate acidizing. Hydroxyethylethylenediaminetetraacetic acid (HEDTA), L-glutamic acid-N, N-diacetic acid (GLDA) and amino polycarboxylic acids (EDTA) are common chelating agents that were used as iron control chemicals. The pH of these chelating agents was in the range of 3–5. They were used in small concentrations due to their limited solubility in spent acid. The sodium salt of erythorbic acid was also used as another iron control agent. Another additive examined was an aqueous fluorochemical surfactant that would provide a durable protective film against oil and water on porous surfaces. In addition, two organic corrosion inhibitors and methanol were tested in

different concentrations. Methanol was additionally used in a methanol extraction procedure for removing the deposited salt, CaCl_2 in the carbonate cores after spent acid injection.

Equipment

Table 3 provides the list of all the equipment used in this study.

Table 3—List of the equipment, brands and models		
Item	Brand	Model
Core Holder	Phoenix Instruments	Triaxial
DSA Instrument	Eurotechnica Ingenieurburo	PD-E700LL-H
Gas Regulator	Swagelok	Medium - high pressure
Back Pressure Regulator	Swagelok	Medium - high pressure
Transducer	Swagelok	S
Pump	Teledyne Isco	500D
Accumulator	Phoenix Instruments	N/A
Oven	Binder	FD 53
Digital Balance	Mettler Toledo	X54035
Helium Porosimeter	Core Lab Instruments	Ultragrain-200TM
Density-meter	Pioneer	N/A
Digital pH-meter	Oakton	PH 510
Water Distillation Machine	Barnstead EasyPure RoDi	N/A
Gas Flow-meter	Omega	FMA1620A
Vacuum Pump	Edwards	RV12
Methanol Extraction Equipment	Prism Research Glass Inc.	N/A

Flow Setup

Fig. 7 is a schematic diagram of the flow setup used for coreflood experiments and permeability measurements. The setup included a core holder that was connected to the nitrogen gas supply with a regulator and an accumulator at the inlet. Inside the core holder there was a rubber sleeve filled with water that was used to apply the overburden pressure (normally 1500 psi) all around the core sample. The liquid was injected from the accumulator using a pump. At the outlet, the core holder was connected to a vacuum pump for evacuating air from the system before liquid saturation. A backpressure regulator was used to adjust the outlet pressure. The liquid was collected in the separator and its weight was measured using a digital balance. A gas flow-meter was also used at the outlet to measure the gas rate. Pressure transducers were placed at the inlet and outlet to record the pressure drop in the system. An oven was used separately from the system to dry the rock after the experiments.

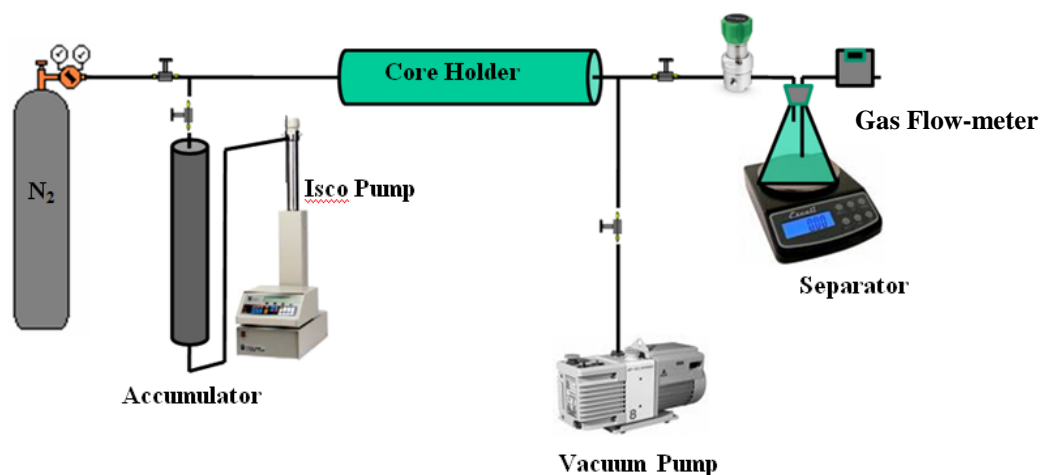


Fig. 7—Flow setup used for coreflood tests.

Spontaneous Liquid Imbibition Setup

A digital balance that is connected to a data acquisition system is used to conduct the spontaneous imbibition experiment. As seen in **Fig. 8**, the dry core was wrapped with a nylon wire and placed on a hook attached to the bottom of the balance. A beaker with a volume relative to the size of the core was used to immerse the rock in liquid. As the rock was immersed in liquid, the weight of the rock was recorded with time by the data acquisition system.

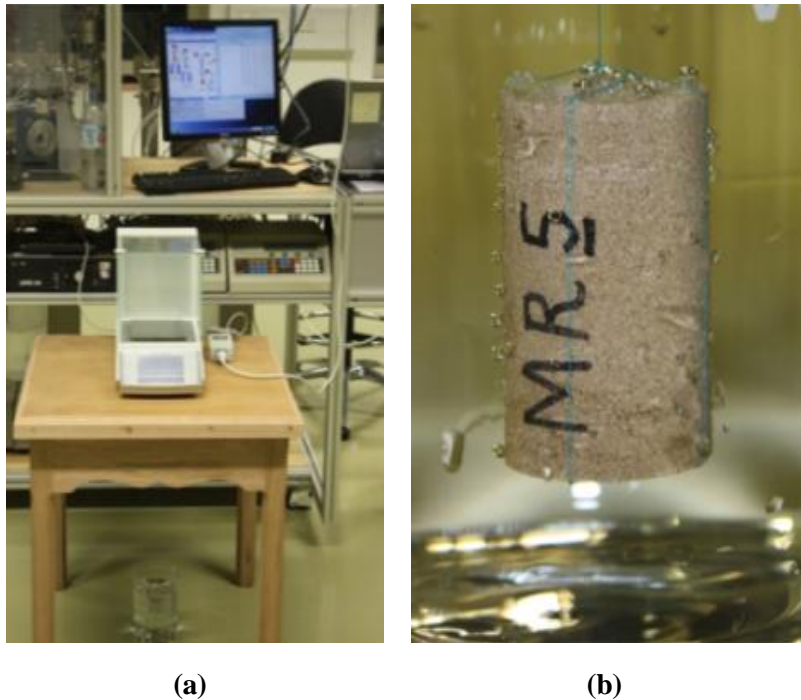


Fig. 8—Spontaneous liquid imbibition setup. (a) The setup consists of a scale connected to the data acquisition system. (b) The dry core was wrapped with a nylon wire under the scale. Air bubbles are observed at the surface as liquid imbibes into the core.

Drop Shape Analysis (DSA) Instrument

A high-pressure/high-temperature drop shape analysis (DSA) instrument was used to measure surface tension and contact angle of the spent acid solutions. **Fig. 9** is a schematic diagram of this equipment. The liquid tank was filled with the spent acid and a pump was used to inject the liquid through the capillary tube (outside diameter = 0.79 mm). The capillary tube was placed inside a cell equipped with a temperature controller and a heating jacket. The liquid-wetted surfaces of the instrument (cell and needle) were made from Hastelloy-C, which can resist corrosion at high temperatures.

The pendant drop for surface tension and sessile drop (on the top of the crystal chip) for contact angle measurements were generated inside the cell. The cell was filled with compressed nitrogen gas; the heating jacket and the temperature controller were used to increase the temperature to the required value. The required pressure inside the cell was set by the gas pressure generator. The image analysis module of the instrument was a Krüss model DSA10-MK2L. A digital camera was used to take the picture of the droplet. This image was then digitized and analyzed by the software.

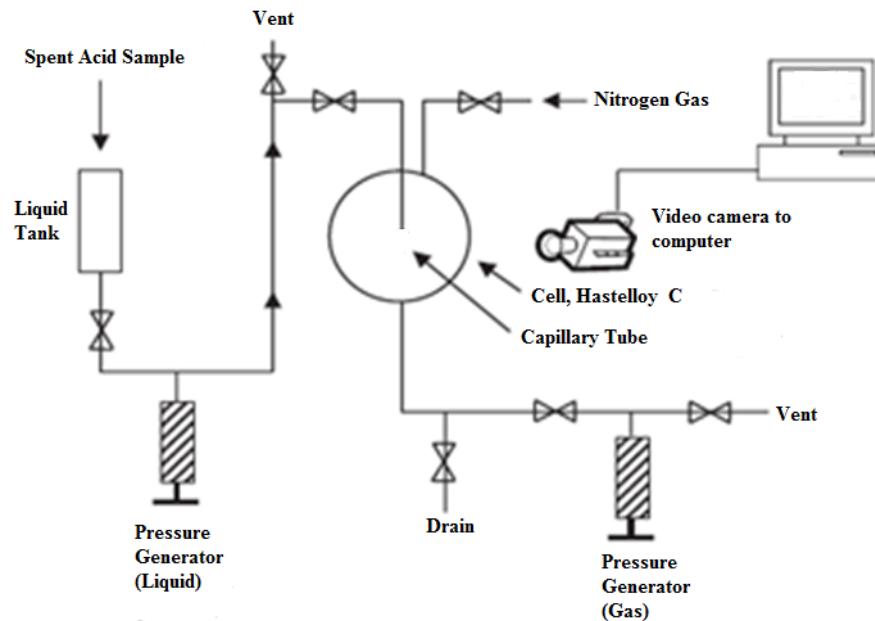


Fig. 9—A schematic diagram of the HT/HP pendant drop instrument.

Helium Porosimeter

The porosity of the core samples was measured using a helium porosimeter. As shown in **Fig. 10**, the setup included a matrix cup and cup assembly which was connected to the helium gas line. The core sample was placed in the matrix cup and spacers in various sizes were used to fill up the remaining space in the cup. The system was equipped with a pressure transducer and was computer controlled. Porosity could be automatically calculated from the entered data (core dimensions, weight, and number of spacers left out).

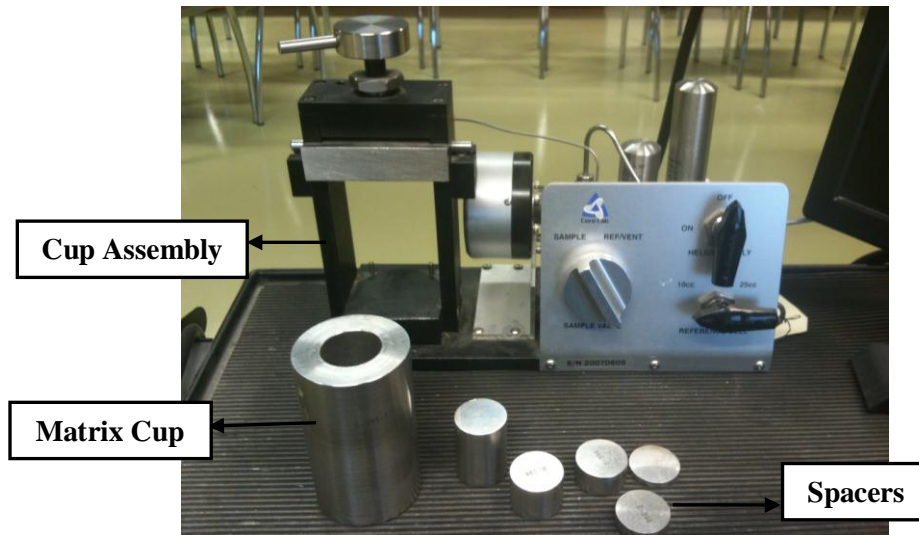


Fig. 10—Helium porosimeter.

Methanol Extraction Equipment

This equipment was used to remove the precipitated salt, CaCl_2 in the rock after spent acid injection. As shown in **Fig. 11**, this setup was comprised of a heater, cooling system, extraction solvent (methanol) flask and condensing column. Vapor of the boiling methanol would enter the rock and remove the salt. Some of the vapor would liquefy in the condensing column and return to the methanol flask. The rest of the vapor would escape to the atmosphere, as the top of the condensing column was open to the air. This cyclic routine would continue until all of the deposited salt was removed, and original weight, permeability and porosity of the rock were regained.

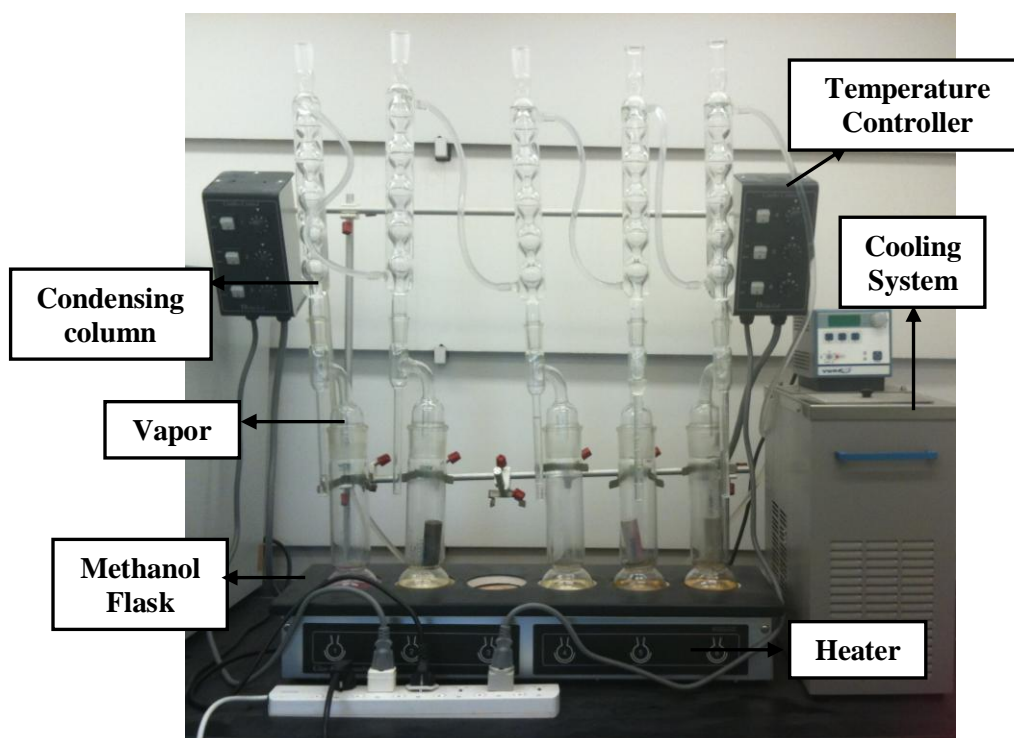


Fig. 11—Methanol extraction equipment.

Densities of spent acid solutions were measured at each temperature and pressure point using a digital density-meter.

The pH of spent acid was measured before every surface tension measurement using a digital pH-meter. This would ensure that the pH was approximately three to four.

A water distillation machine was used to transform tap water into pure distilled water for use in the experiments.

Procedure

Porosity Measurements

In order to measure porosity, pore spaces fraction in the core sample, the following steps were taken:

1. Measure the dimensions and weight of the dry core sample.
2. Place the core inside the matrix cup and fill it up with the spacers.
3. Record the number and size of the spacers left out.
4. Load the matrix cup into the cup assembly.
5. Start the helium porosimeter software and enter core data.
6. Charge the system with helium gas by opening and closing the helium valve and record gas pressure, P_1 .
7. Position valve to expand helium gas into the matrix cup and record gas pressure again, P_2 .
8. The software uses the data to calculate porosity by **Eq. 5** and **Eq. 6**:

$$P_1 V_1 = P_2 (V_1 + V_d + V_s - V_m) \dots\dots\dots (5)$$

$$\phi = \frac{V_b - V_m}{V_b} \dots\dots\dots (6)$$

where V_1 is the volume of the matrix cup, V_d is the dead volume inside the matrix cup, V_s is the volume of the spacers left out, V_m is the matrix (rock solid particles) volume, ϕ is the porosity, V_p is the pore volume, and V_b is the total or bulk volume.

Permeability Measurements

Permeability is the measure of the ease with which a fluid can flow through a porous medium. To calculate this rock property, the Darcy equation is generally used. **Eq. 7** is used for calculating effective permeability in the case of liquid flow (Economides 1994).

$$q = \frac{-k A}{\mu} \frac{dp}{dl} \dots\dots\dots (7)$$

where k is the permeability, $\frac{dp}{dl}$ is the pressure gradient, A is the cross sectional area, q is the flow rate, and μ is the viscosity of the fluid.

The darcy equation can be derived for gas flow as well. At standard conditions and assuming ideal gas behavior, **Eq. 8** can be used to calculate gas effective permeability (Economides *et al.* 1994).

$$q = \frac{-k A}{\mu} \frac{P_2^2 - P_1^2}{2L} \dots\dots\dots (8)$$

where P_1 is the inlet pressure and P_2 is the outlet pressure.

In this study absolute permeability was acquired when the core sample was 100% saturated with gas. Absolute permeability is obtained when there is only one fluid phase present (in this case, gas). In order to obtain the permeability of core samples the following steps were taken:

1. Measure weight of the dry core.
2. Apply 1500 psi overburden pressure.
3. Connect the nitrogen gas line to the inlet and the gas flow-meter to the outlet of the core holder.
4. Use the gas pressure regulator at the inlet to set the pressure between 120 to 140 psi.
5. Use the gas pressure regulator at the outlet to set the pressure at 60 psi.
6. Record gas flow rate.
7. Repeat above steps, increasing the outlet pressure by 10 psi.

8. Continue until the pressure difference between inlet and outlet pressures is 10-20 psi.
9. In an Excel spread sheet, plot q/A versus $(P_1^2 - P_2^2)/2L$ to form a linear relationship. The slope of the line is equal to k/μ .
10. Permeability is calculated by multiplying the slope of the line by the gas viscosity.

Spontaneous Liquid Imbibition

Imbibition is the process of absorbing a wetting phase into a porous medium with time. This experiment can be used to evaluate rock wettability such that a higher fluid imbibition level would mean more wetting-phase wettability. For example, if the wetting phase is water, the higher the water imbibition level is, the more water-wetting the rocks are.

The following procedure was followed for the imbibition experiment:

1. Measure the dry weight of the core.
2. Wrap the core with nylon wire; make a loop at the end of the wire and place it on the hook attached to the bottom of the digital balance.
3. Record the weight of the core with wire in the data acquisition system.
4. Fill a clean beaker with enough liquid; while the data logging is running, immerse the core in the liquid.
5. At the beginning, log weight every 2 seconds and after a few minutes increase logging interval time. For over-night imbibition tests (about 20 hours), the logging is every 5 minutes.

6. At the end of the experiment, remove the core from the beaker and measure its weight with wire.
7. Put the core sample in the oven. After it is completely dried, record its weight.
8. The liquid saturation of the core with time is then calculated and plotted in an Excel spread sheet. The saturation is calculated using the following equations:

$$W_{ai} = W_{af} - (W_{rf} - W_{ri}) \dots\dots\dots (9)$$

$$S_l(t) = \frac{W_a(t) - W_{ai}}{g\rho V_p} \dots\dots\dots (10)$$

Here, $W_a(t)$ is the apparent weight of the core at each time step, W_{ai} is the initial apparent weight (obtained from **Eq. 9**), S_l is the liquid saturation, W_{af} is the final apparent weight of the core, W_{rf} is the final real dry weight of the core, W_{ri} is the initial real dry weight of the core, g is the gravitational acceleration, ρ is the density of the liquid, and V_p is the pore volume of the sample.

Relative Permeability Endpoints

For wettability and capillarity analysis relative permeability end points are measured. This is more convenient than obtaining the relative permeability curves, as that procedure is laborious and time consuming. Relative permeability end points are shown by green circles on **Fig. 12**. Point 1 corresponds to the irreducible water saturation and maximum gas relative permeability and point 2 corresponds to the maximum possible water saturation and maximum water relative permeability.

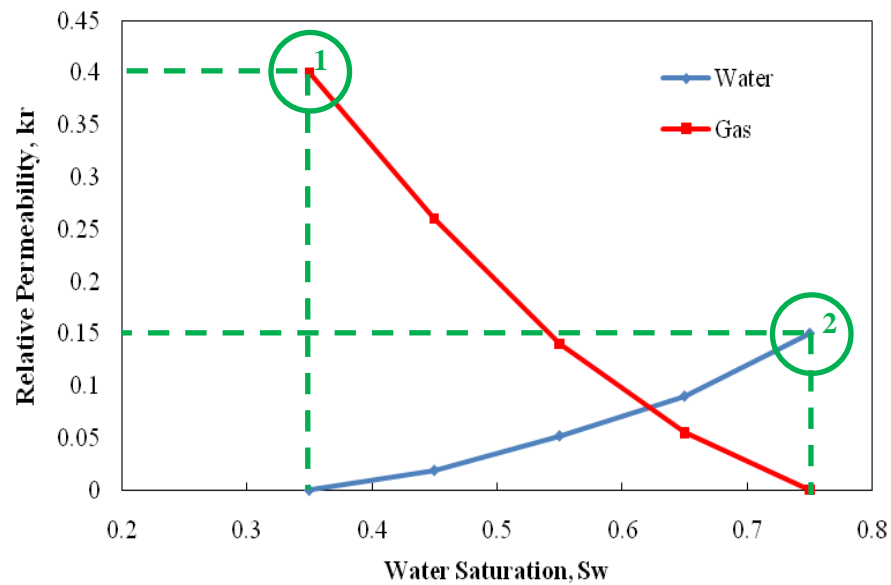


Fig. 12—Typical gas-water relative permeability plot; corresponding relative permeability end points.

The following steps were taken for measuring the relative permeability end points:

1. Clean and dry the core flood setup.
2. Weigh the dry core sample.
3. Pack the rock in the core holder and apply 1500 psi overburden pressure.
4. Fill the accumulator with the liquid (water or spent acid) and connect the liquid line to the inlet. Keep the liquid valve closed.
5. Connect the vacuum line to the outlet. Open the valve and start vacuuming. Vacuum for at least 2 hours.

6. Turn off and disconnect the vacuum. Open the valve at the inlet that is connected to the liquid line.
7. Inject liquid at a constant pressure of 200 psi, until the pressure in the core holder stabilizes.
8. In case of spent acid, the rock was aged for about three hours in the fluid inside the core holder.
9. Unpack the rock and measure its weight.
10. Pack the rock back in the core holder.
11. Connect the nitrogen gas line to the inlet and the gas flow meter to the outlet.
12. Inject gas at a rate of 0.2 cc/min for at least 20 hours. Take flow meter and inlet pressure readings frequently.
13. Once finished, unpack the rock and measure its weight.
14. If the injected liquid is spent acid, put the rock immediately in the methanol extraction setup. Leave it until all the deposited salt, CaCl_2 is removed and the original dry weight, porosity, and permeability (after drying in the oven) are recovered (normally 48 hours).
15. If the injected liquid is water, put the rock in the oven to dry.

With the apparent weight recorded in steps 8 and 12, and the dry weight of the core sample, maximum water saturation and irreducible liquid saturation can be calculated using the following equation:

$$S_1 = \frac{W_a - W_{\text{dry}}}{g\rho V_p} \dots\dots\dots (11)$$

In order to calculate liquid and gas relative permeability values, the following equations are used:

$$k_{rl} = \frac{k_l}{k_a} \dots\dots\dots (12)$$

$$k_{rg} = \frac{k_g}{k_a} \dots\dots\dots (13)$$

where k_{rl} and k_{rg} are the liquid and gas relative permeability, k_l and k_g are the effective liquid and gas permeability when there is more than one fluid phase present, and k_a is the absolute permeability.

Surface Tension Measurements

Surface tension measurements were carried out by generating a pendant drop at the end of the capillary tube (outside diameter = 0.79 mm) inside the cell filled with compressed nitrogen gas, **Fig. 9**. The heating jacket surrounding the cell and the temperature controller were used to increase the temperature to the required value. When the temperature or pressure was changed, the pendant drop was left to reach equilibrium for 10–15 min before taking the measurements. An image of the drop was recorded using the digital camera and its shape was extracted in the image analysis module of the instrument, as shown in **Fig. 13**. The digitized drop shape was used along with processing techniques to build an accurate interfacial profile of the pendant drop. Liquid and gas densities were also used to calculate the surface tension in the software.

The density of nitrogen gas as a function of temperature and pressure was obtained from Lemmon (2001). Densities of spent acid solutions were measured at each temperature and pressure point using the digital density-meter. The pH of spent acid was

measured before every surface tension measurement using the digital pH-meter in order to ensure that the pH is approximately three to four.

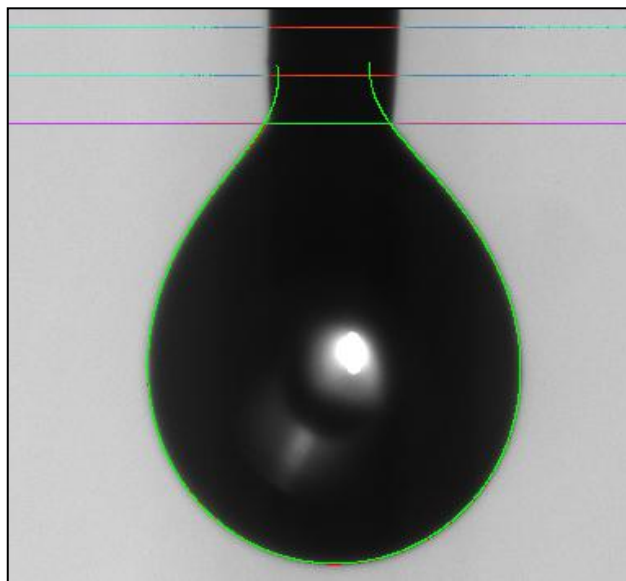


Fig. 13—Pendant drop image extracted and digitized by the image analysis software. The top two horizontal lines are used to estimate the volume of the capillary tube and the bottom line is used to determine top of the droplet.

At the beginning and the end of each experiment, the system was thoroughly flushed with distilled water. In the case of using a corrosion inhibitor, acetone was also used to clean the instrument. For quality control and to calibrate the system, the surface tension of distilled water was measured and compared to the values in the literature. A good agreement was set to obtain with the data produced by Álvarez *et al.* (1997) and Nasr-El-Din (2004).

Contact Angle Measurements

The same DSA instrument used for surface tension measurements of a pendant drop, was used to measure contact angle by sessile and captive drop methods. To conduct accurate contact angle measurements, calcite crystal chips were polished to provide a smooth and homogeneous surface for contact angle measurements. A crystal chip was put inside the cell and a droplet of spent acid was placed on the top of it, through the capillary tube. The temperature and pressure were adjusted to obtain the required values. When the temperature or pressure was changed, the sessile drop was left to reach equilibrium for approximately one hour before taking the measurements. An image of the drop was recorded using the digital camera and the drop shape was extracted in the image analysis module of the instrument, **Fig. 14**. The right and left angles between the base line and the tangent at the drop boundaries were determined.

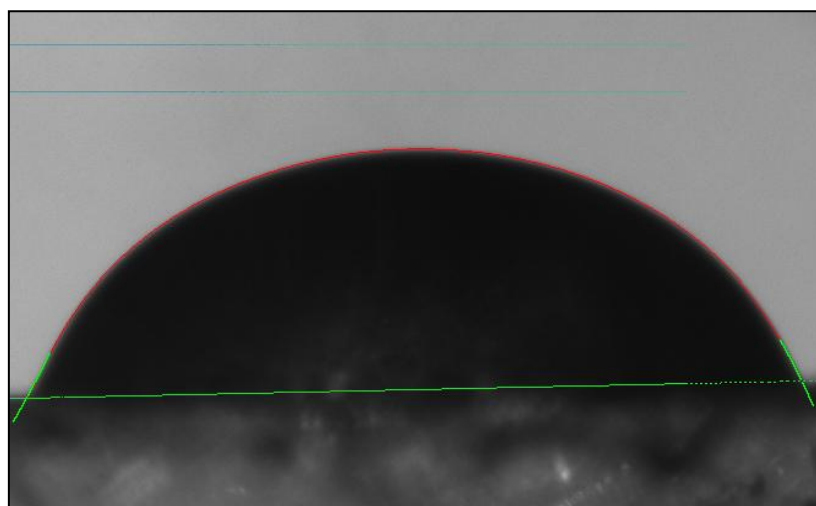


Fig. 14—Sessile drop image extracted and digitized by the image analysis software.

As in the surface tension experiments, the pH of the spent acid was measured before every contact angle measurement using a digital pH-meter in order to ensure that the pH was approximately three to four. At the beginning and the end of each experiment, the system was thoroughly flushed with distilled water. In the case of using a corrosion inhibitor, acetone was also used to clean the instrument.

Spent Acid Preparation

To prepare the spent acid, amounts of calcium chloride (CaCl_2) and water needed were calculated according to the balanced chemical reaction equation between calcium carbonate (CaCO_3) and 15 wt.% HCl, **Eq. 1**.

When formic acid was used for relative permeability endpoint experiments, the acid was separately spent and then added to the spent HCl acid solution. In order to spend formic acid, the amount needed was collected in a beaker and then pieces of carbonate rocks were added to it until the reaction stopped, **Fig. 15**. Final pH was measured to be between three and four.



Fig. 15—Spending formic acid in a beaker by adding pieces of carbonate rock.

CHAPTER III

RESULTS AND DISCUSSIONS

To study the effect of common acid additives on capillarity, the main reason behind spent acid trapping, surface tension and contact angle of spent acid fluids were tested using the DSA instrument. In addition, the overall impact of some of these chemicals on carbonate wettability characteristics was further evaluated by conducting spontaneous water imbibition tests and obtaining irreducible liquid saturation before and after treatment. The following are the results of this study.

Surface Tension Experiments

Surface tension of spent acid with no additives was measured at various temperatures, ranging from 20 °C to 150 °C.

As shown in **Fig. 16**, increase in temperature had a decreasing effect on the surface tension of spent acid. At room temperature, surface tension was measured to be around 76 mN/m while at 150 °C it decreased by 60% to 30 mN/m.

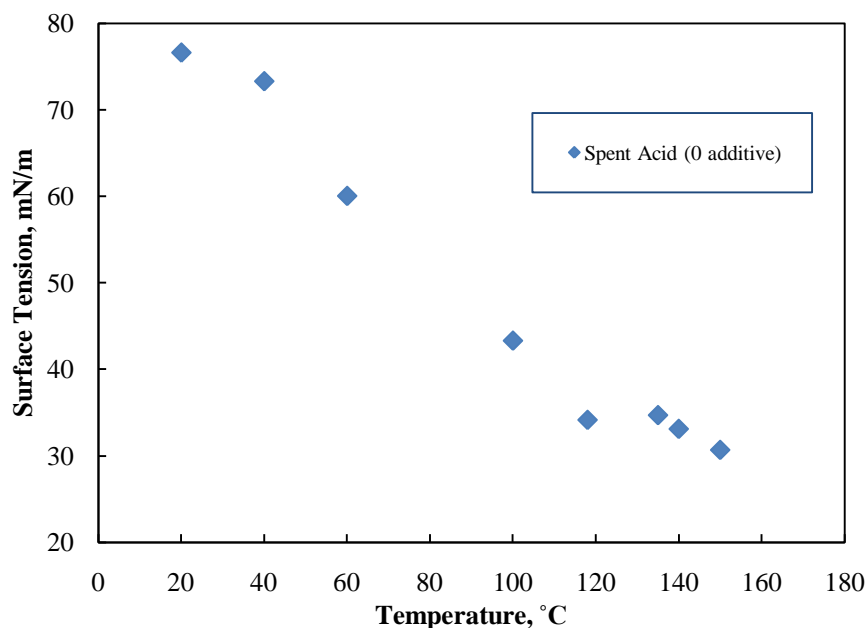


Fig. 16—Effect of temperature on surface tension of spent HCl acid with no additives at 1000 psi.

Different acid additives were added to the spent acid solution and their surface tension in spent acid was individually measured and compared to the surface tension of spent acid with no additives. **Fig. 17** shows the surface tension measurements for different concentrations of methanol in spent acid. It can be seen that an increase in concentration of methanol decreased the surface tension. This change was more evident when a higher concentration was used. Also at low temperatures, the reduction in surface tension was greater than at higher temperatures. The decreasing trend of surface tension with increase in temperature was seen for spent acids with all concentrations of methanol used.

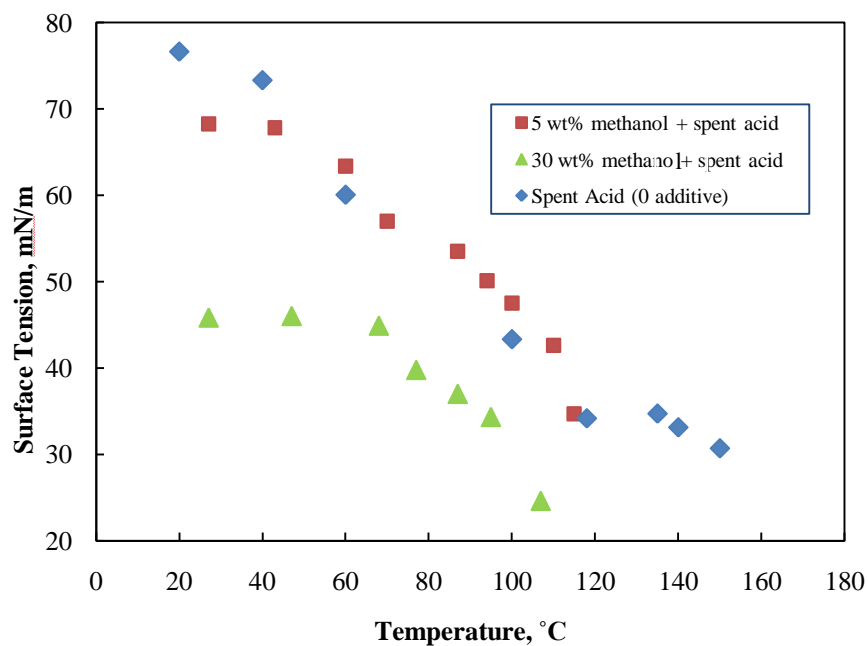


Fig. 17—Effect of methanol on surface tension of spent acid at 1000 psi.

Results for inhibitor I showed that this corrosion inhibitor decreased surface tension, **Fig. 18**. At higher concentration, and at lower temperature, the reduction in surface tension was greater. The results for inhibitor II also indicated a reducing impact on surface tension. However, increase in its concentration showed no impact on surface tension, as the measurements for 0.2 and 2 wt.% inhibitor II were very similar, **Fig. 19**. The reduction in surface tension in the case of inhibitor II was greater than when Inhibitor I was used. For both corrosion inhibitors, increasing temperature exhibited the same decreasing impact on the surface tension.

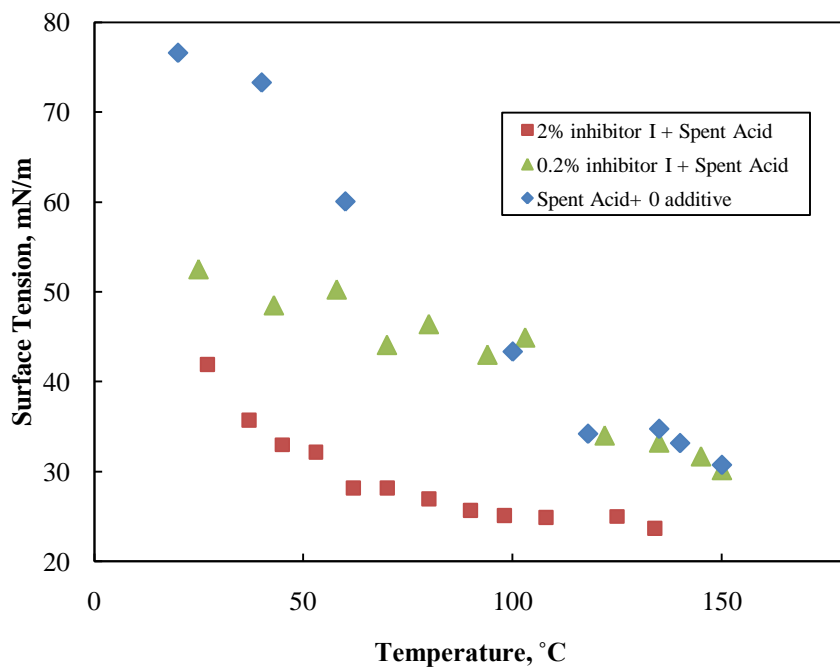


Fig. 18—Effect of inhibitor I on surface tension of spent acid at 1000 psi.

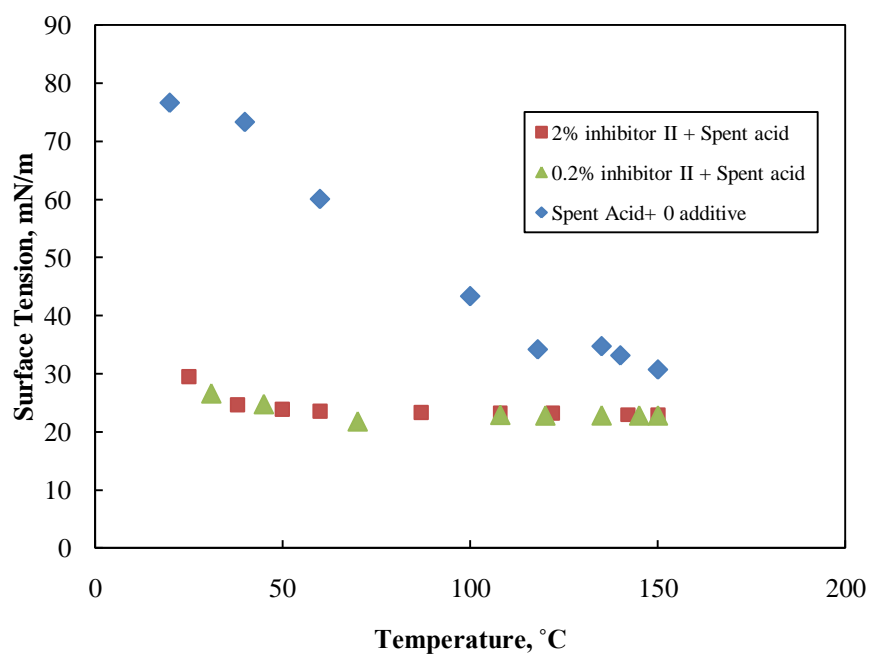


Fig. 19—Effect of inhibitor II on surface tension of spent acid at 1000 psi.

HEDTA and GLDA were also tested as the two common iron control agents. Results illustrated that both of these acid additives did not have a significant effect on the surface tension of spent acid, **Fig. 20** and **Fig. 21**.

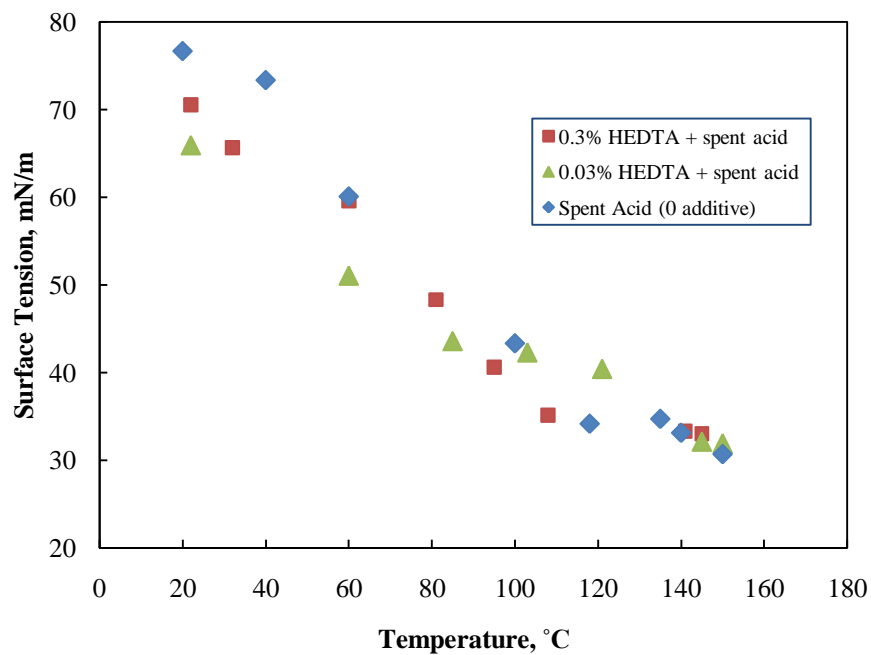


Fig. 20—Effect of HEDTA on surface tension of spent acid at 1000 psi.

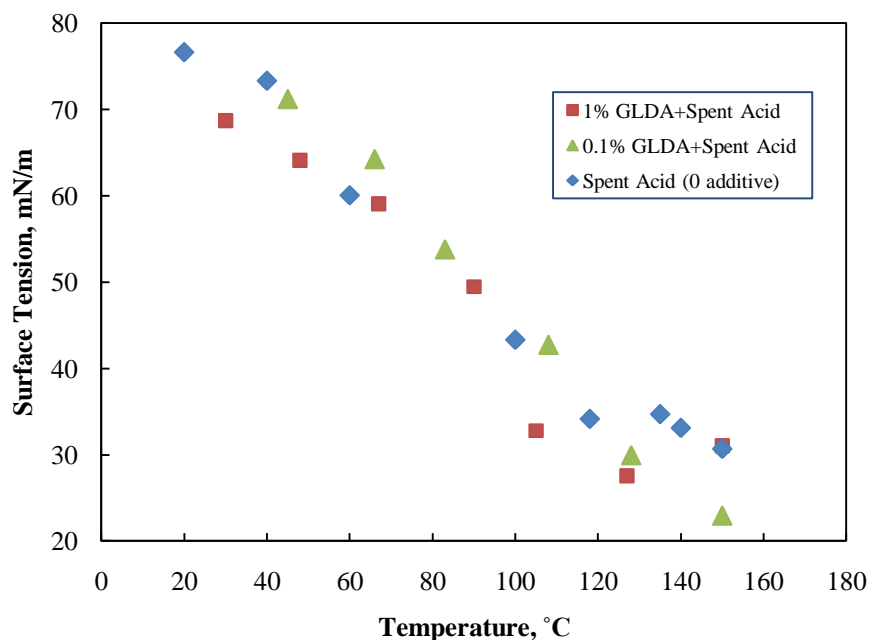


Fig. 21—Effect of GLDA on surface tension of spent acid at 1000 psi.

Live formic acid was added at different concentrations, up to 10 wt.%, to spent HCl acid and surface tension measurements were conducted at 150 °C and 1000 psi. As it is shown in **Fig. 22**, no change in surface tension of spent acid was observed as a result of the addition of formic acid. The values of surface tension for spent HCl with formic acid were also very similar to the values of surface tension for distilled water and spent acid with no additives. Therefore, it can be said that formic acid did not change the surface tension of spent acid.

In the case of acetic acid (live), a higher concentration of 30 wt.% was also used but it exhibited similar behavior in spent HCl as formic acid, as shown in **Fig. 23**. This confirms that addition of organic acids to spent acid will not affect the surface tension and recovery of spent acid.

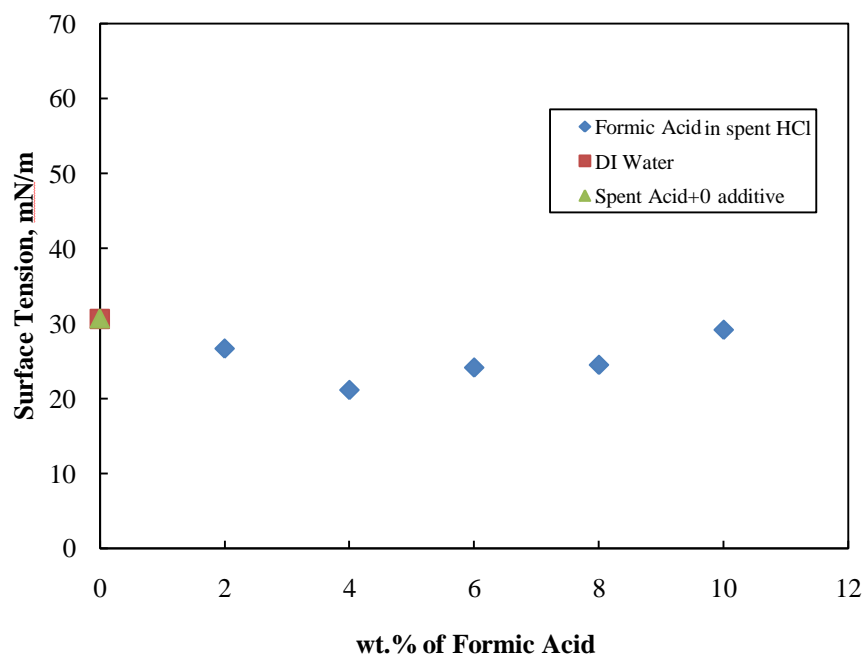


Fig. 22—Effect of formic acid on surface tension of spent acid at 150 °C and 1000 psi.

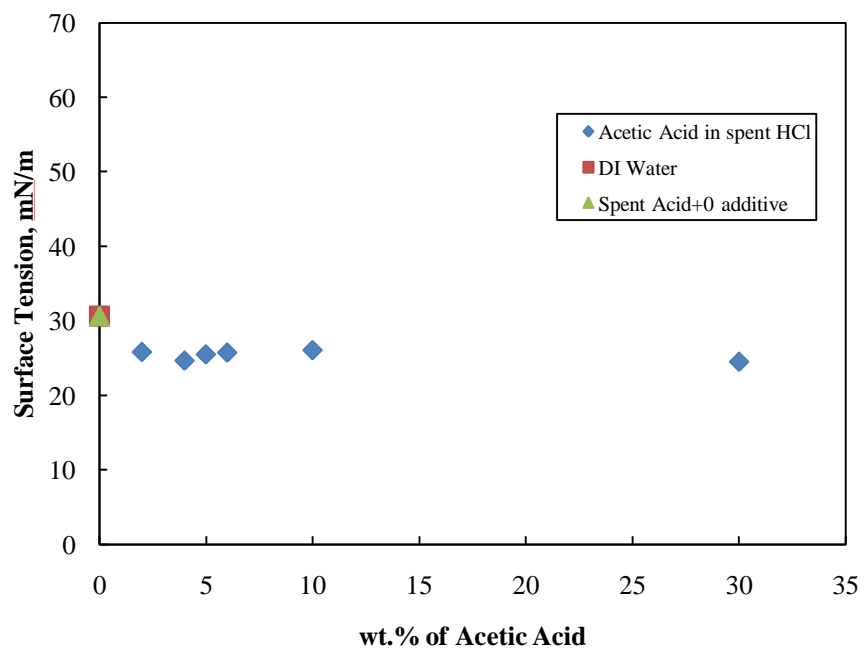


Fig. 23—Effect of acetic acid on surface tension of spent acid at 150 °C and 1000 psi.

An attempt was made to test surface tension of spent acid with a mutual solvent as well, but due to the high salinity of spent acid, EGMBE was not soluble at any of the concentrations used.

Contact Angle Experiments

The effect of several acid additives on the contact angle of 15 wt.% spent HCl was evaluated. The droplet of spent acid was placed on the surface of calcite crystal chip inside the cell heated to 100 °C and pressurized to 1000 psi. Droplet images and contact angle measurements were taken frequently until the droplet was stabilized and the contact angle measurements were constant. This would usually take from 1 to 2 hours. **Fig. 24** shows droplet images taken at the beginning of a contact angle experiment and after 2 hours. As it is evident, there is a major variation in the contact angle when the droplet is stabilized.

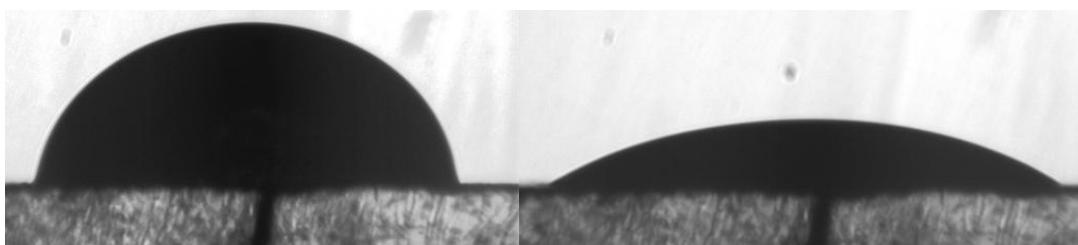


Fig. 24—Stabilized spent acid droplet after 2 hours. The left image shows the first image taken at the beginning of the experiment and the left image shows the same droplet after two hours.

Fig. 25 shows the contact angle measurements for two different concentrations of methanol in spent acid with the crystal surface. It can be seen that an increase in

concentration of methanol decreased the contact angle. This change was more evident when a higher concentration was used.

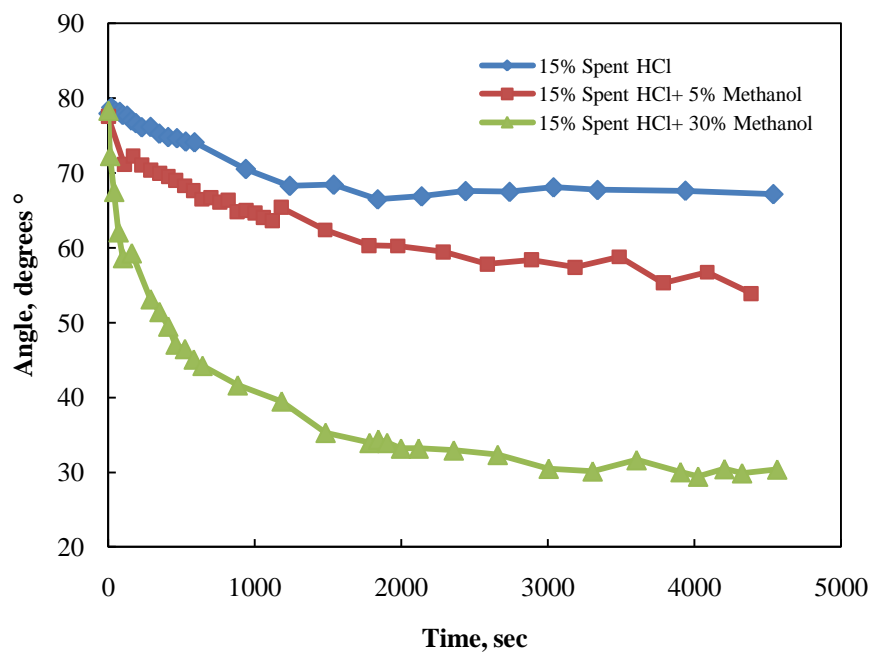


Fig. 25—Effect of methanol on contact angle of spent acid at 100 °C & 1000 psi.

Acetic acid and formic acid had a decreasing impact on contact angle, **Fig. 26** and **Fig. 27**. Increase in acetic acid concentration showed a greater change in contact angle while increase in formic acid concentration did not have a significant impact.

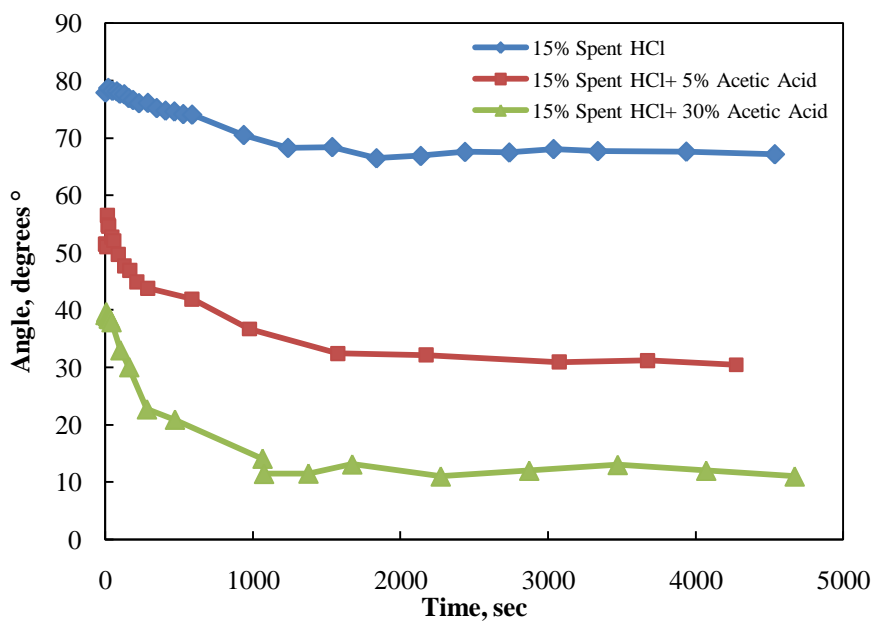


Fig. 26—Effect of acetic acid on contact angle of spent acid at 100 °C & 1000 psi.

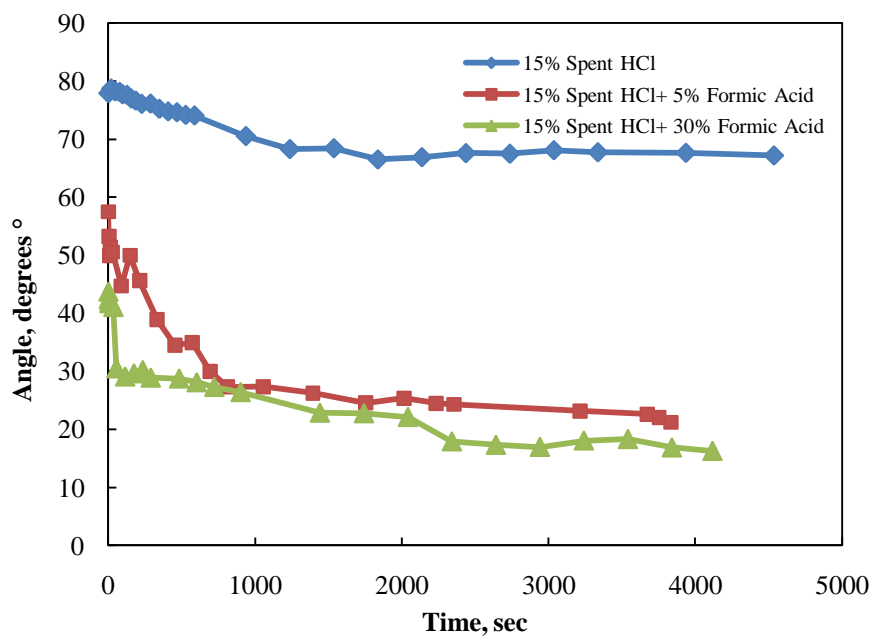


Fig. 27—Effect of formic acid on contact angle of spent acid at 100 °C & 1000 psi.

Fig. 28 and Fig. 29 show the results for the two iron control agents. Both HEDTA and GLDA showed no impact on contact angle at a concentration of 0.3 wt.%, while at the lower concentration of 0.03 wt.% they decreased the contact angle by 70% and 40%, respectively. This is probably due to the chemical interactions at the fluid-solid surface interfaces that need to be studied further.

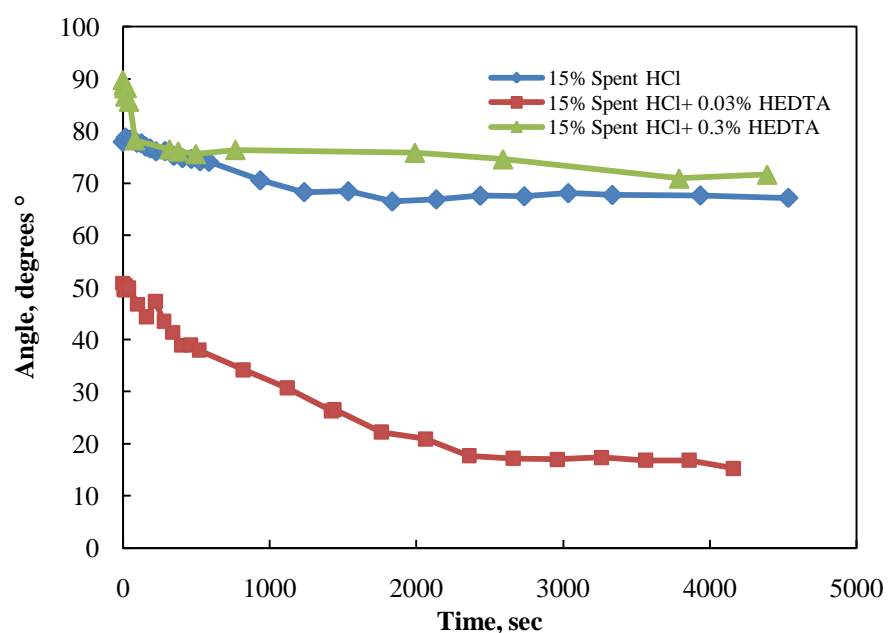


Fig. 28—Effect of HEDTA on contact angle of spent acid at 100 °C & 1000 psi.

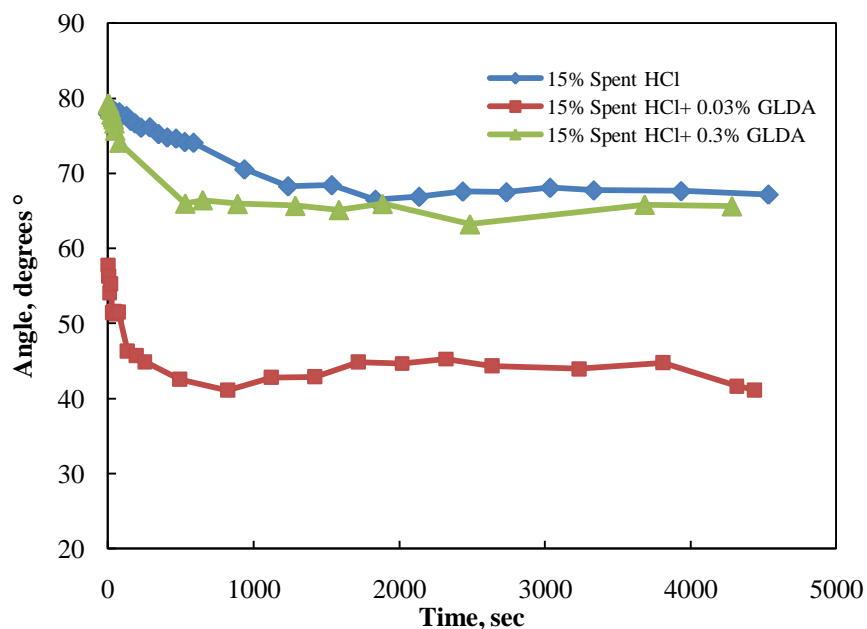


Fig. 29—Effect of GLDA on contact angle of spent acid at 100 °C & 1000 psi.

Corrosion inhibitors I and II, at both concentrations, in spent acid spread immediately on the surface of calcite crystal and the software was not able to extract the drop shape. Visually analyzed, the contact angle for both corrosion inhibitors was estimated to be around 10 degrees after stabilization. A difference in concentration did not affect contact angle significantly. **Fig. 30** shows contact angle images of spent acid with 0.2 wt.% inhibitor I. The top image was taken immediately when the droplet was placed on the crystal surface and the bottom image was taken after approximately 5 seconds.

An attempt was also made to test the contact angle of spent acid with mutual solvent, but due to the limited solubility of EGMBE in spent acid that was not possible.

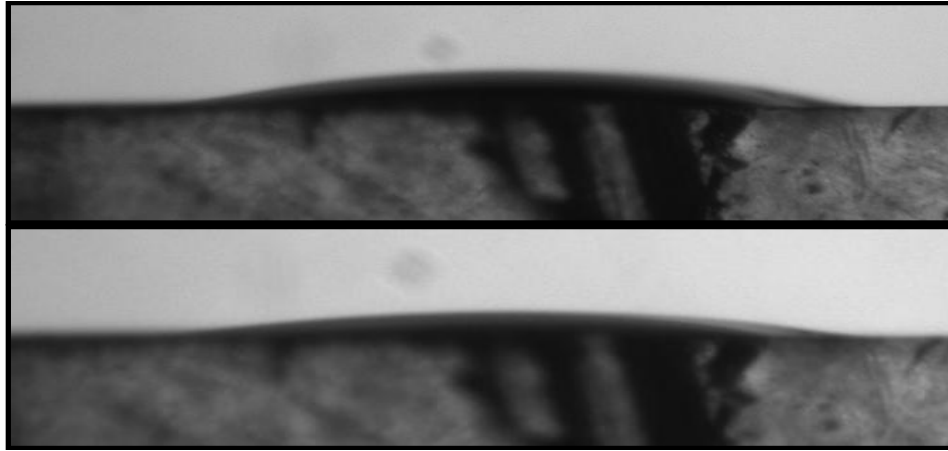


Fig. 30—Sessile drop images of spent acid with 0.2 wt.% inhibitor I for contact angle analysis. Top image was taken immediately when the droplet was placed on crystal surface and bottom image was taken after approximately 5 seconds.

Spontaneous Water Imbibition and Irreducible Saturation Tests

Effect of Spent HCl on Wettability

The effect of different concentrations of spent HCl on wettability was tested on core samples with 3 inches length. Water imbibition tests were conducted for two core samples, MR10 and MR11, treated with 15 wt.% and 28 wt.% spent HCl, respectively. The imbibition curves for these two core samples were compared to the imbibition curve for an untreated core sample of the same size, **Fig. 31**. Results show that different concentrations of spent HCl had no impact on the water imbibition rate and wettability, as the imbibition curves for both treated cores were very similar to the one for the original core sample.

In addition, it can be seen that the maximum water saturation that was reached in the untreated rock after 17 hours of imbibition was only about 47%. Normally, in a strongly water-wet rock, a water saturation of about 60% is expected after a few hours of imbibition time. This shows that the original wettability of the rock was not strongly water-wetting.

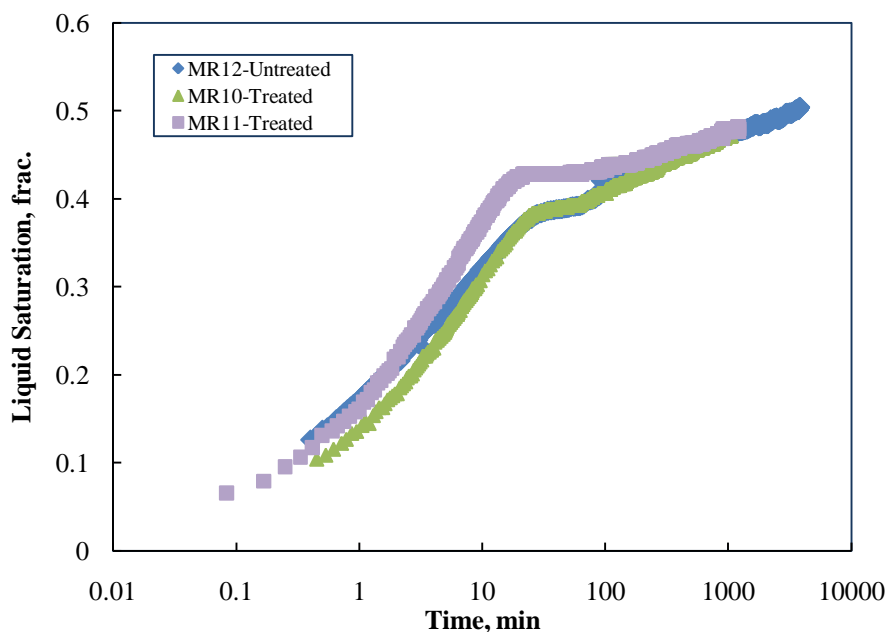


Fig. 31—Spontaneous water imbibition for untreated and treated core samples with 15 wt.% and 28 wt.% spent HCl.

Effect of Various Acid Additives on Wettability

The earlier study on the effect of different commonly used acid additives on surface tension and contact angle of carbonate rocks showed that some of the acid additives such as methanol reduce both the surface tension and the contact angle. As

previously explained, based on **Eq . 2**, the reduction in the surface tension was favorable as it would result in a lower capillary pressure but the reduction in the contact angle was unfavorable since it would lead to a higher capillary pressure and more spent acid trapping. This illustrated the need for a more comprehensive study to confirm the full impact of these additives on the wettability of the carbonate rocks.

In addition to the spontaneous imbibition test, an important parameter to study in wettability analysis is the irreducible wetting-phase saturation. Thus, the objectives of this part of the work were set to be: 1) study the impact of at least two of the acid additives that were tested previously (in surface tension and contact angle experiments) on the irreducible spent acid saturation; and 2) run imbibition tests before and after spent acid exposure to check for any long-term wettability changes as a result of the exposure to the additives.

Table 4 lists the names of the different core samples used, the treatments and the experiments conducted in each case.

Table 4—List of all core samples used, the treatments and experiments conducted in each case

Core Sample	Treatment	Experiment
MR10	15 wt.% spent HCl	Imbibition
MR11	28 wt.% spent HCl	Imbibition
MR12	15 wt.% spent HCl + 4 wt.% fluorochemical surfactant	Imbibition & Core flood
MR33	15 wt.% spent HCl + 1 wt.% fluorochemical surfactant	Imbibition
ILS6	15 wt.% Spent HCl + 0.3 wt.% Sodium Erythorbate	Imbibition
ILS11	15 wt.% Spent HCl + 0.3 wt.% EDTA	Imbibition
ILS21	15 wt.% Spent HCl + 5 wt.% Formic Acid	Imbibition & Core flood
ILS23	15 wt.% Spent HCl + 5 wt.% methanol	Imbibition & Core flood

Core flood experiments were conducted for ILS21 and ILS23 in order to obtain irreducible liquid saturations before and after treatment. In each case the spent acid was left in the rock for about 3 hours for aging purposes. Irreducible water saturation ($S_{w_{ir}}$) was acquired for the untreated rock, and irreducible spent acid saturation ($S_{s_{ir}}$) was obtained by injecting nitrogen gas at constant pressure for about 20 hours into the core sample that was fully saturated with the spent acid solution.

Results listed in **Table 5** show that formic acid reduced the irreducible fluid saturation by approximately 35%. This would result in smaller capillary pressure and

therefore better recovery of spent acid. Reduction in irreducible saturation also showed that wettability of the rock was changed into less water wetting.

On the other hand, when 5 wt.% methanol was used in spent acid irreducible liquid saturation increased by 12%. Thus, methanol had an overall increasing impact on the capillary pressure and would cause more trapping of the spent acid. This was also an indication of wettability change towards more water wetting, as expected based on the results of the contact angle experiments. Therefore, the impact of methanol on the contact angle was more dominant than its impact on the surface tension in affecting capillarity characteristics.

Table 5—Results of irreducible liquid saturation for ILS21 and ILS23		
Core Name	Sw_{ir} (%) – Original	Ss_{ir} (%) – After Treatment
ILS21	53.7	35.72
ILS23	54.29	60.81

Fig. 32 and **Fig. 33** show the water imbibition tests for ILS21 and ILS23 before and after exposure to the spent acid. As can be seen in these figures, the liquid saturation over time was the same before and after spent acid exposure in both cases. Therefore, wettability characteristics of the rocks were regained and rocks were not permanently affected by either formic acid or methanol.

Wettability of several other additives was also evaluated using spontaneous water imbibition tests. The result of the imbibition test for the core sample ILS6 that was

treated with sodium erythorbate shows that this acid additive does not have an impact on the rock wettability, **Fig. 34**.

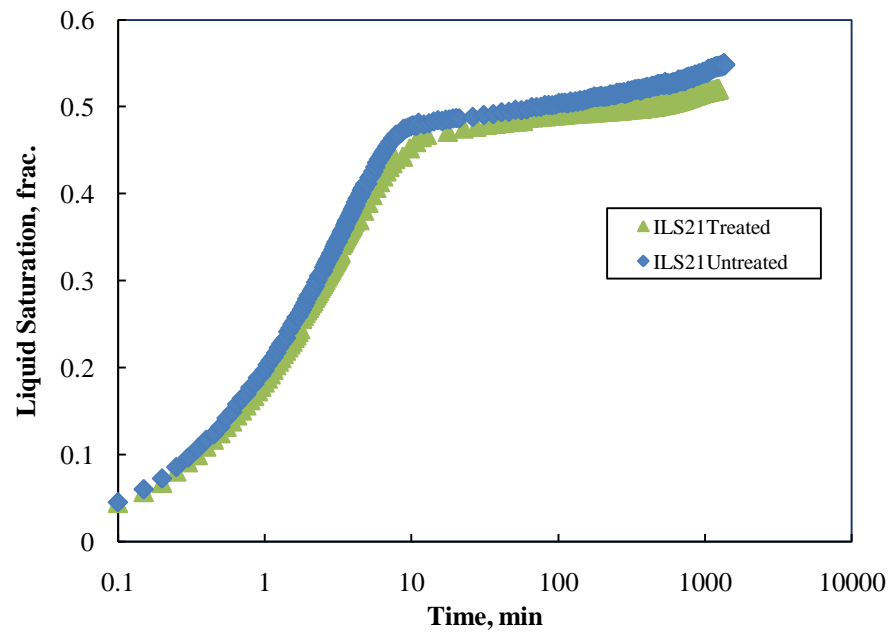


Fig. 32—Spontaneous water imbibition for untreated and treated ILS21 with 5 wt.% formic acid in 15 wt.% spent HCl acid.

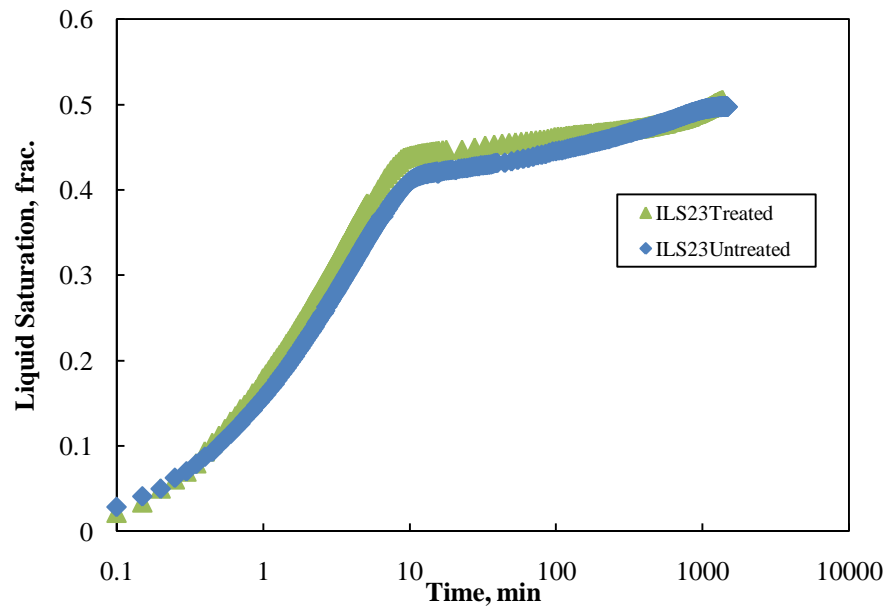


Fig. 33—Spontaneous water imbibition for untreated and treated ILS23 with 5 wt.% methanol in 15 wt.% spent HCl acid.

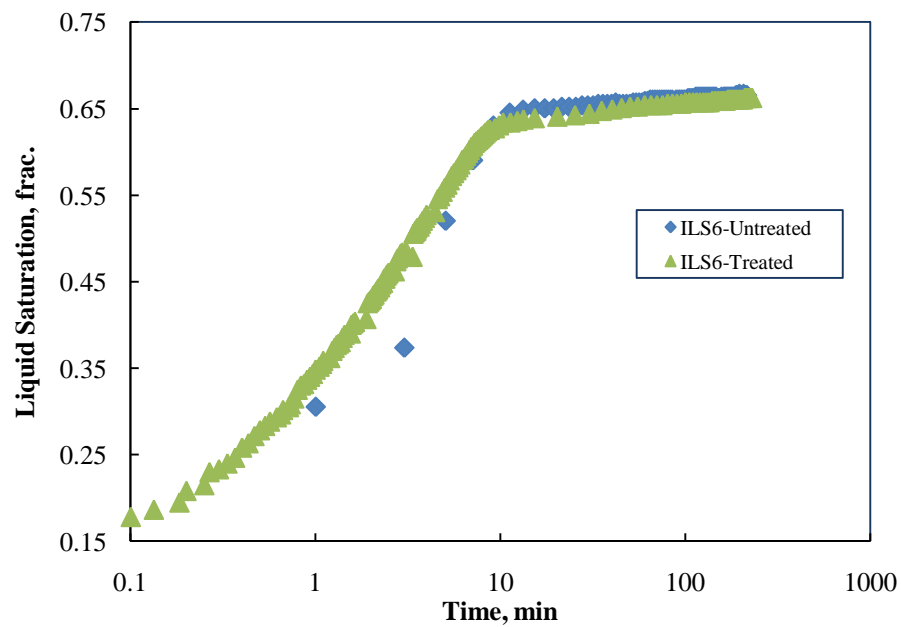


Fig. 34—Spontaneous water imbibition for untreated and treated ILS6 with 0.3 wt.% sodium erythorbate in 15 wt.% spent HCl acid.

Furthermore, the result of the test with EDTA on ILS11 is shown in **Fig. 35**. It can be seen that this additive does not have a significant impact on the rock wettability, similar to what was seen with other chelating agents tested.

The fluorochemical surfactant was tested in two concentrations, 1 and 4 wt.% in spent HCl using core samples MR33 and MR12, respectively. The result of the imbibition test with 4 wt.% of this chemical is shown and compared to the imbibition curve of the untreated rock in **Fig. 36**. The reduction in the imbibition rate and water saturation shows that this chemical alters wettability into more gas-wetting.

Similar results were obtained when using a lower concentration (1%) of this additive.

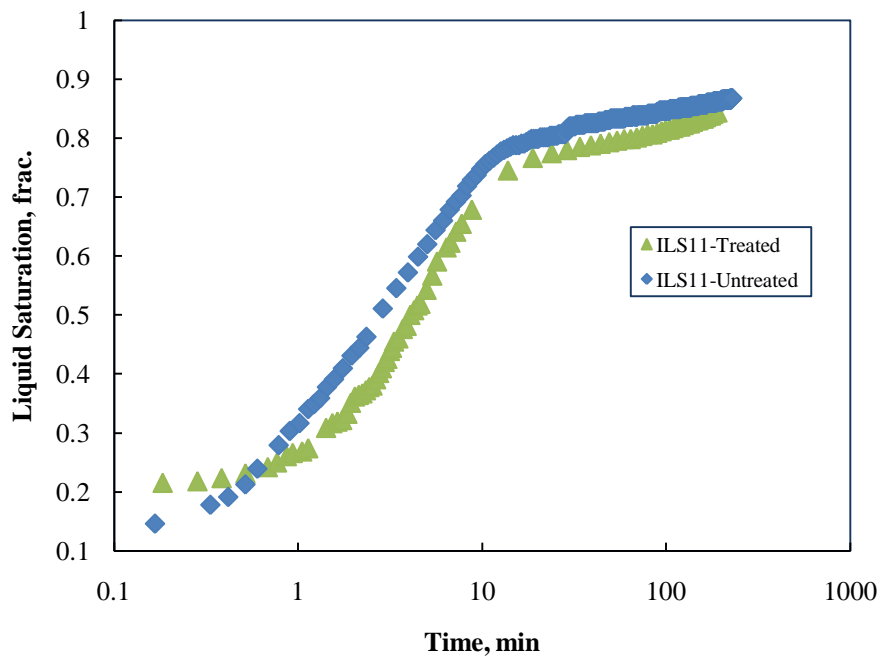


Fig. 35—Spontaneous water imbibition for untreated and treated ILS11 with 0.3 wt.% EDTA in 15 wt.% spent HCl acid.

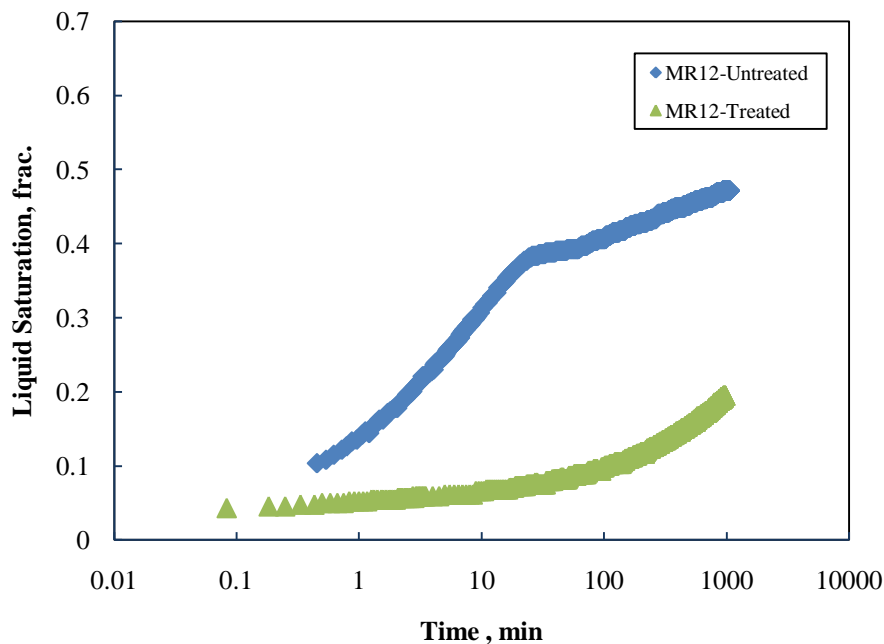


Fig. 36—Spontaneous water imbibition for untreated and treated MR12 with 4 wt.% fluorochemical surfactant in 15 wt.% spent HCl acid.

A core flood test was conducted to study the effect of the fluorochemical surfactant on the irreducible liquid saturation and gas relative permeability. **Fig. 37** shows the acquired relative permeability end points for the untreated and treated (with 1 wt.% of fluorochemical surfactant) core sample MR33. As the result of using this chemical, irreducible liquid saturation decreased from 53% to 50% and gas relative permeability increased from 0.64 to 0.8 (about 25%). This confirms the previous finding from the imbibition test; fluorochemical surfactants alter wettability to less water-wetting.

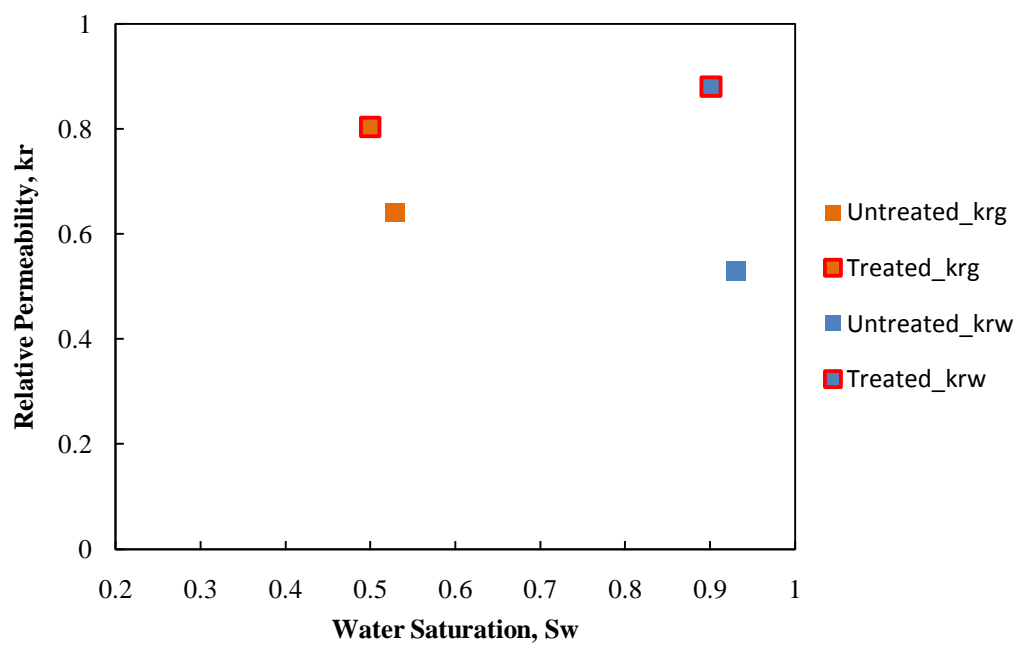


Fig. 37—Effect of wettability change on gas relative permeability and irreducible liquid saturation in case of using 1% fluorochemical surfactant in 15 wt.% spent HCl acid using MR33.

CHAPTER IV

CONCLUSIONS

The following is the concluding remarks of the study on the effect of various common acid additives on carbonate rock wettability and capillarity characteristics in low permeability gas carbonate reservoirs. It also includes the conclusions drawn from several core flood experiments and spontaneous water imbibition tests conducted in this work.

1. Surface tension of spent acid with/without additives decreases with increasing temperature at constant pressure.
2. Methanol reduces surface tension of spent acid. This change is more evident when a higher concentration of methanol is used.
3. Inhibitors I and II reduce surface tension of spent acid. Increase in concentration of inhibitor I further reduces the surface tension, but increase in inhibitor II concentration does not affect the surface tension. The reduction in surface tension in the case of inhibitor II is greater than when inhibitor I was used.
4. HEDTA and GLDA do not affect the surface tension of spent acid.
5. Addition of organic acids, formic and acetic acid, to spent acid does not affect the surface tension of spent acid.
6. Increasing temperature up to 100 °C increases contact angle, while beyond this temperature contact angle is decreased. Contact angle behavior with temperature is not consistent at all temperatures.

7. Increase in concentration of methanol in spent acid decreases the contact angle. This change is more evident when a higher concentration is used.
8. Organic acids, formic and acetic acids, decrease contact angle of spent acid with the crystal surface. Increase in acetic acid concentration show a greater change in contact angle while increase in formic acid concentration does not have a significant impact.
9. Corrosion inhibitors decrease the contact angle of spent acids with the surface of calcite crystal chip. Inhibitors I and II, at both concentrations, in spent acid, spread immediately on the surface of calcite crystal and the software was not able to extract the drop shape.
10. Mutual solvent, EGMBE is not soluble in spent acid at any concentrations due to the high salinity of spent acid.
11. Acid additives can diversely affect the surface tension and contact angle (wettability) of carbonate rocks. Reduction in the surface tension is favorable as it will result in lower capillary pressure but the reduction in the contact angle is unfavorable as it will lead to a higher capillary pressure and more spent acid trapping. Selection of different acid additives and the concentrations used should be according to the knowledge of their impact on the rock capillarity characteristics.
12. The overall impact of formic acid on capillary pressure and carbonate rock wettability was studied. Formic acid decreases the capillary pressure at the gas-liquid interface and therefore changes the wettability of the rocks temporarily to

less water-wetting.

13. Methanol increases the capillary pressure at the gas-liquid interface in carbonate rocks and changes the wettability of the rocks temporarily to more water-wetting.
14. The impact of methanol on the contact angle is more dominant than its impact on the surface tension in affecting capillarity characteristics.
15. Using Formic acid in acidizing will result in better recovery of spent acid while using methanol will cause more trapping of spent acid in tight reservoirs.
16. The surfaces of the core samples used were water-wet, but they are not considered as strongly water-wet.
17. Different concentrations of spent HCl have no impact on the capillary pressure and rock wettability.
18. EDTA and sodium erythorbate have no impact on capillary pressure and carbonate rock wettability.
19. The fluorochemical surfactant changes the rock wettability into more gas wetting. Use of this chemical will help in recovering spent acid.
20. The irreducible liquid saturation for core samples with permeability of 2-3 md and with applied pressure gradient of 3.28 psi/cm is approximately 54%.
21. The effect of the additives on wettability of the rocks will exist only as long as the rock is in contact with the solution. There is no permanent (or long-term) impact on wettability as a result of using most of the acid additives.
22. Fluorochemical surfactant forms a film on the rock surface and therefore it will have a long-term impact on wettability.

23. Wettability changes due to spent acid invasion can increase or decrease productivity depending on the type of additives used.
24. It is necessary to study the impact of different acid additives on the wettability before every acid job as this would help in better designing the acid formulae and enhance well productivity by minimizing capillarity.

REFERENCES

- Al-Mutairi, S.H., Nasr-El-Din, H.A., Al-Muntasheri, G.A., and Aldriweesh, S.M. 2005. Corrosion Control during Acid Fracturing of Deep Gas Wells: Lab Studies and Field Cases. Paper SPE 94639 presented at the SPE International Symposium on Oilfield Corrosion, Aberdeen, United Kingdom, 13 May. doi: 10.2118/94639-MS.
- Álvarez, E., Vázquez, G., Sánchez-Vilas, M., Sanjurjo, B., and Navaza, J.M. 1997. Surface Tension of Organic Acids + Water Binary Mixtures from 20 °C to 50 °C. *J. Chem. Eng. Data* **42** (5): 957 – 960.
- Anderson, W.G. 1987. Wettability Literature Survey-Part 5: The Effects of Wettability on Waterflooding. *SPE J. of Pet Tech* **39** (12): 1453 – 1468. doi: 10.2118/16471-PA.
- Bazin, B. and Abdulahad, G. 1999. Experimental Investigation of Some Properties of Emulsified Acid Systems for Stimulation of Carbonate Formations. Paper SPE 53237 presented at the Middle East Oil Show and Conference, Bahrain, 20 – 23 February. doi: 10.2118/53237-MS.
- Bazin, B., Bieber, M.T., Roque, C., and Bouteica, M. 1996. Improvement in the Characterization of the Acid Wormholing By "In Situ" X-Ray Ct Visualizations. Paper SPE 31073 presented at the SPE Formation Damage Control Symposium, Lafayette, Louisiana, 14 – 15 February. doi: 10.2118/31073-MS.
- Bennion, D.B., Thomas, F.B., and Bietz, R.F. 1996. Low Permeability Gas Reservoirs: Problems, Opportunities and Solutions for Drilling, Completion, Stimulation and Production. Paper SPE 35577 presented at the SPE Gas Technology Symposium, Calgary, Alberta, Canada, 28 April – 1 May. doi: 10.2118/35577-MS.
- Bennion, D.B., Thomas, F.B., and Ma, T. 2000. Formation Damage Processes Reducing Productivity of Low Permeability Gas Reservoirs. Paper SPE 60325 presented at the SPE Rocky Mountain Regional/Low-Permeability Reservoirs Symposium and Exhibition, Denver, Colorado, 12 – 15 March. doi: 10.2118/60325-MS.
- Buijse, M., Boer, P.D., Breukel, B., and Burgos G. 2004. Organic Acids in Carbonate Acidizing. *SPE Prod & Oper* **19** (3): 128 – 134. doi: 10.2118/82211-PA.
- Buijse, M. and Glasbergen, G. 2005. A Semiempirical Model To Calculate Wormhole Growth in Carbonate Acidizing. Paper SPE 96892 presented at SPE Annual

Technical Conference and Exhibition, Dallas, Texas, USA, 9–12 October. doi: 10.2118/96892-MS

Butler, M., Trueblood, J.B., Pope, G.A., and Sharma, M. 2009. A Field Demonstration of a New Chemical Stimulation Treatment for Fluid-Blocked Gas Wells. Paper SPE 125077 presented at the SPE Annual Technical Conference and Exhibition, New Orleans, Louisiana, USA, 4–7 October. doi: 10.2118/125077-MS.

Cassidy, J.M., McNeil, R.I., and Kiser, C. 2007. Understanding Formic Acid Decomposition as a Corrosion Inhibitor Intensifier in Strong Acid Environments. Paper SPE 106185 presented at the International Symposium on Oilfield Chemistry, Houston, Texas, 8 February – 2 March. doi: 10.2118/106185-MS.

Churcher, P.L., French, P.R., Shaw, J.C., and Schramm, L.L. 1991. Rock Properties of Berea Sandstone, Baker Dolomite, and Indiana Limestone. Paper SPE 21044 presented at the SPE International Symposium on Oilfield Chemistry, Anaheim, California, 20 – 22 February. doi: 10.2118/21044-MS.

Dabbousi, B., Nasr-El-Din, H.A., and Al-Muhaish, A. 1999. Surface Tension of Stimulation Fluids. SPE 50732 presented at the SPE Oilfield Chemistry, Houston, TX, February 16 – 19. doi: 10.2118/50732-MS.

Daccord, G., Touboul, E., and Lenormand, R. 1989. Carbonate Acidizing: Toward a Quantitative Model of the Wormholing Phenomenon. *SPE Prod Eng* **4** (1): 63 – 68. doi: 10.2118/16887-PA.

Economides, M. J., Hill, A. D., and Ehlig-Economides C. 1994. *Petroleum Production Systems*. Englewood Cliffs, New Jersey: Prentice Hall.

Fahes, M.M. and Firoozabadi, A. 2007. Wettability Alteration to Intermediate Gas-Wetting in Gas-Condensate Reservoirs at High Temperatures. *SPE J.* **12** (4): 397 – 407. doi: 10.2118/96184-PA.

Fredd, C.N. and Fogler, H.S. 1998. The Influence of Equilibrium Reactions on the Kinetics of Calcite Dissolution in Acetic Acid Solutions. *Chem. Eng. Sci.*, **53** (22): 3863 – 3874.

Fredd, C.N. and Fogler, H.S. 1999. Optimum Conditions for Wormhole Formation in Carbonate Porous Media: The Influence of Transport and Reaction. *SPE J.*: 196 – 205.

Frenier, W.W., Growcock, F.B. and Lopp, V.R. 1988. Mechanisms of Corrosion Inhibitors Used in Acidizing Wells. *SPE Prod. Eng.* **3** (4): 584 – 590. doi: 10.2118/14092-PA.

- Hall, B.E. 1975. The Effect of Mutual Solvents on Adsorption in Sandstone Acidizing. *J. Pet. Tech.* **27**: 1439 – 1442.
- Hellberg, P.E. 2011. Environmentally Acceptable Polymeric Corrosion Inhibitors. Paper presented at the SPE International Symposium on Oilfield Chemistry, The Woodlands, Texas, USA, 11 – 13 April. doi: 10.2118/140780-MS.
- Huang, T., Hill, A.D. and Schechter, R.S. 1997. Reaction Rate and Fluid Loss: The Keys to Wormhole Initiation and Propagation in Carbonate Acidizing. Paper SPE 37312 presented at the International Symposium on Oilfield Chemistry, Houston, Texas, 18 – 21 February. doi: 10.2118/37312-MS.
- Huang, T., McElfresh, P.M. and Gabrysch, A.D. 2003. Carbonate Matrix Acidizing Fluids at High Temperatures: Acetic Acid, Chelating Agents or Long-Chained Carboxylic Acids. Paper SPE 82268 presented at the SPE European Formation Damage Conference, The Hague, Netherlands, 13 – 14 May. doi: 10.2118/82268-MS.
- Hung, K.M., Hill, A.D. and Sepehrnoori, K. 1989. A Mechanistic Model of Wormhole Growth in Carbonate Matrix Acidizing and Acid Fracturing. *SPE J. Pet Tech* **41** (1): 59 – 66. doi: 10.2118/16886-PA.
- King, G.E. and Lee, R.M. 1988. Adsorption and Chlorination of Mutual Solvents Used in Acidizing. *SPE Prod Eng* **3** (2): 205 – 209. doi: 10.2118/14432-PA.
- Lemmon, E.W., McLinden, M.O. and Friend, D.G. 2001. Thermophysical properties of fluid systems. In: Linstrom, P.J., Mallard, W.G. (Eds.), NIST Chemistry WebBook, NIST Standard Reference Database Number 69. National Institute of Standards and Technology, Gaithersburg, MD 20899. <http://webbook.nist.gov>.
- Li, K. and Firoozabadi, A. 2000. Experimental Study of Wettability Alteration to Preferential Gas-Wetting in Porous Media and Its Effects. *SPE Res Eval & Eng* **3** (2): 139–149. doi: 10.2118/62515-PA.
- Nasr-El-Din, H.A, Al-Othman, A.M., Taylor, K.C. and Al-Ghamdi, A.H. 2004. Surface Tension of HCl-based Stimulation Fluids at High Temperatures. *J. Pet Sci. Eng.* (43): 57–73.
- Nasr-El-Din, H.A., Driweesh, S.M. and Muntasheri, G.A. 2003. Field Application of HCl-Formic Acid System to Acid Fracture Deep Gas Wells Completed with Super Cr-13 Tubing in Saudi Arabia. Paper SPE 84925 presented at the SPE International Improved Oil Recovery Conference in Asia Pacific, Kuala Lumpur, Malaysia, 20 – 21 October. doi: 10.2118/84925-MS.

- Penny, G.S., Soliman, M.W., and Briscoe, J.E. 1983. Enhanced Load Water Recovery Technique Improves Stimulation Results. Paper SPE 12149 presented at the SPE Annual Technical Conference and Exhibition, San Francisco, California, USA, 5–8 October. doi: 10.2118/12149-MS.
- Randles, J.E.B. and Schiffrin, D.J. 1965. Surface Tension of Dilute Acid Solutions. *J. Phys. Chem.* **62**: 2403–2408.
- Schechter, R.S. 1992. *Oil Well Stimulation*, Englewood Cliffs, New Jersey: Prentice Hall.
- Sengul, M. and Remisio, L.H.A. 2002. Applied Carbonate Stimulation:- an Engineering Approach. Paper SPE 78560 presented at the Abu Dhabi International Petroleum Exhibition and Conference, Abu Dhabi, United Arab Emirates. 13-16 October. doi: 10.2118/78560-MS.
- Shukla, S., Zhu, D. and Hill, A.D. 2003. Gas Assisted Acidizing of Carbonate Formations. Paper SPE 82273 presented at the SPE European Formation Damage Conference, The Hague, Netherlands, 13 – 14 May. doi: 10.2118/82273-MS.
- Tang, G.Q. and Firoozabadi, A. 2002. Relative Permeability Modification in Gas/Liquid Systems Through Wettability Alteration to Intermediate Gas Wetting. *SPE Res Eval & Eng* **5** (6): 427–436. doi: 10.2118/81195-PA.
- Travaloni-Louvisse, A.M., Saliba, C.M., Manier, F.B., Franco, Z.A., Rodrigues, V.F. and González, G. 1990. The Use of Ethanol in Oil Well Stimulation Fluids. *J. Pet. Sci. Eng.* **4** (3): 257–272.
- Wang, W. and Gupta, A. 1995. Investigation of the Effect of Temperature and Pressure on Wettability Using Modified Pendant Drop Method. Paper SPE 30544 presented at the SPE Annual Technical Conference and Exhibition, Dallas, TX, USA, 22–25 October. doi: 10.2118/30544-MS.
- Wang, Y., Hill, A.D. and Schechter, R.S. 1993. The Optimum Injection Rate for Matrix Acidizing of Carbonate Formations. Paper SPE 26578 presented at the SPE Annual Technical Conference and Exhibition, Houston, Texas, 3 – 6 October. doi: 10.2118/26578-MS.
- Weissenborn, P.K. and Pugh, R.J. 1996. Surface Tension of Aqueous Solutions of Electrolytes: Relationship with Ion Hydration, Oxygen Solubility, and Bubble Coalescence. *J. Colloid Interface Sci.* **184** (2): 550–563.

VITA

Name: Mehrnoosh Saneifar

Address: Texas A&M, University at Qatar
Education City
Doha, Qatar

Email Address: m_saneifar@yahoo.com

Education: B.S., Petroleum Engineering, Texas A&M University at Qatar,
May 2009

M.S., Petroleum Engineering, Texas A&M University, August 2011